

FY02 ENGINEERING TECHNOLOGY REPORTS

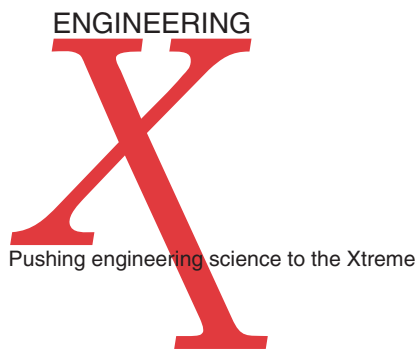
Volume 2 :

LDRD



**MARCH
2003**





Acknowledgments

Scientific Editing

Camille Minichino

Graphic Design

Irene J. Chan

Art Production/Layout

Jeffrey Bonivert

Debbie A. Marsh

Kathy J. McCullough

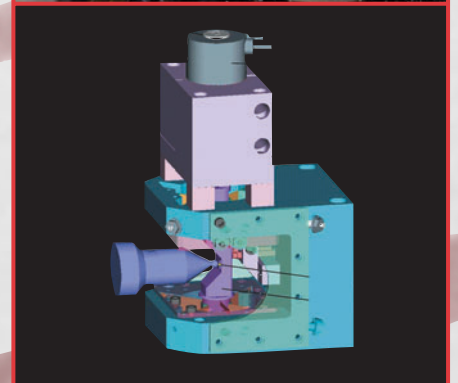
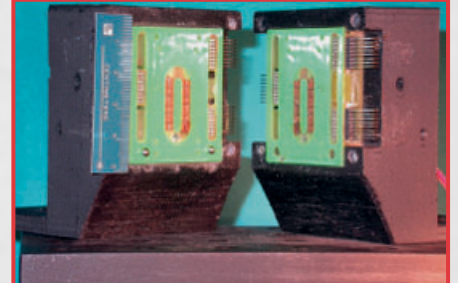
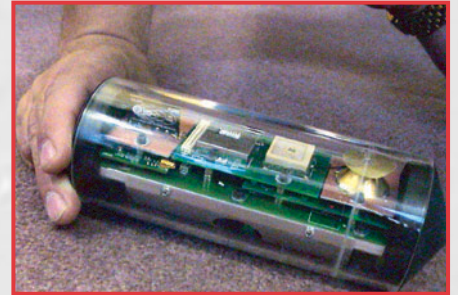
Cover:

Graphics representing LDRD projects from Engineering's Technology Centers.

FY02 ENGINEERING TECHNOLOGY REPORTS

Volume 2 :

LDRD



**MARCH
2003**



Introduction

Jens Mahler iii

Center for Complex Distributed Systems

Cooperative Mobile Sensing Networks

R. S. Roberts, K. A. Kent, E. D. Jones, G. H. Armstrong 3

Ultrawideband Communications

F. Dowla, A. Spiridon, D. Benzel, T. Rosenbury 4

Developing Smart Seismic Arrays: A Simulation Environment, Observational Database, and Advanced Signal Processing

P. E. Harben, D. B. Harris, S. C. Myers, S. C. Larsen, K. E. Nelson 5

Infrastructure Response to Natural and Man-Made Ground Motions: High-Performance Computing and Distributed Sensing for Regional Scale Prediction and Response

D. B. McCallen, S. C. Larsen, A. J. Rodgers 6

Center for Computational Engineering

Numerical Technology for Large-Scale Computational Electromagnetics

R. M. Sharpe, D. A. White, N. J. Champagne, M. Stowell 9

Generalized Methods for Finite-Element Interfaces

M. A. Puso, E. Zywick 10

Higher-Order, Mixed Finite-Element Methods for Time-Domain Electromagnetics

N. K. Madsen, D. A. White, N. J. Champagne 11

Exploratory Research into the Extended Finite-Element Method

R. M. Sharpe, K. D. Mish 12

Modeling and Characterization of Recompressed Damaged Materials

R. Becker 13

Dynamic Simulation Tools for the Analysis and Optimization of Novel Filtration, Sample Collection, and Preparation Systems

D. S. Clague, T. H. Weisgraber, K. D. Ness 14

Center for Microtechnology

Reconfigurable, Optical Code-Division Multiple Access for Fiber-Optic Networks

S. W. Bond, R. J. Welty, I. Y. Han, C. V. Bennett, E. M. Behymer, V. R. Sperry, S. J. Yoo 17

Modeling Tools Development for the Analysis and Design of Photonic Integrated Circuits

T. C. Bond, J. K. Kallman, G. H. Khanaka 18

Disposable Polymerase Chain Reaction Device

E. K. Wheeler, W. Bennett, K. D. Ness, P. Stratton, A. Chen, A. Christian, J. Richards, T. H. Weisgraber 19

Integrated Microfluidic Fuel Processor for Miniature Power Sources

R. S. Upadhye, J. D. Morse, A. F. Jankowski, M. A. Havstad 20

Nanoscale Fabrication of Mesoscale Objects

R. P. Mariella Jr., A. Rubenchik, G. Gilmer, M. Shirk 21

Low-Voltage Spatial Light Modulator

A. P. Papavasiliou 22

Center for Nondestructive Characterization

High-Accuracy X-Ray Imaging of High-Energy-Density Physics Targets

W. Nederbragt, D. Schneberk, T. Barbee, J. L. Klingmann, S. G. Lane, J. A. Jackson25

Ultrasonic Nondestructive Evaluation of Multilayered Structures

M. J. Quarry, K. Fisher, J. L. Rose26

Radial Reflection Diffraction Tomography

S. K. Lehman, S. J. Norton27

Center for Precision Engineering

Extremely High-Bandwidth, Diamond-Tool Axis for Weapons-Physics Target Fabrication

R. C. Montesanti, D. L. Trumper, J. L. Klingmann31

Other Technologies

Hyperspectral Image-Based Broad-Area Search

D. W. Paglieroni35

Author Index

.....37

Introduction

Jens Mahler, Acting Associate Director for Engineering

This report summarizes the science and technology research and development efforts in Lawrence Livermore National Laboratory's Engineering Directorate for FY2002, and exemplifies Engineering's 50-year history of developing the technologies needed to support the Laboratory's missions. Engineering has been a partner in every major program and project at the Laboratory throughout its existence and has prepared for this role with a skilled workforce and the technical resources developed through venues like the Laboratory Directed Research and Development Program (LDRD). This accomplishment is well summarized by Engineering's mission: "To make programs succeed today and to ensure the vitality of the Laboratory tomorrow."

Engineering's investment in new technologies is carried out through two programs, the "Tech Base" program (Volume I) and the LDRD program (Volume II). This report summarizes the LDRD portion of Engineering's Technology Program. LDRD is the vehicle for researching and developing those technologies and competencies that are cutting edge, or that require a significant level of research, or contain some unknown that needs to be fully understood. Tech Base is used to apply those technologies, or adapt them to a Laboratory need. The term commonly used for Tech Base projects is "reduction to practice." Therefore, the LDRD report covered here has a strong research emphasis. Areas that are presented all fall into those needed to accomplish our mission. For FY2002, Engineering's LDRD projects were focused on mesoscale target fabrication and characterization, development of engineering computational capability, material studies and modeling, remote sensing and communications, and microtechnology for national security applications.

Engineering's five Centers, in partnership with the Division Leaders and Department Heads, are responsible for guiding the long-term science and technology investments for the Directorate. The Centers represent technologies that have been identified as critical for the present and future work of the Laboratory, and are chartered to develop their respective areas. Their LDRD projects are the key resources to attain this competency, and, as such, nearly all of Engineering's portfolio falls under one of the five Centers. The Centers and their leaders are:

- Center for Complex Distributed Systems:
Donald J. Meeker, Acting Center Leader
- Center for Computational Engineering:
Robert M. Sharpe
- Center for Microtechnology:
Raymond P. Mariella, Jr.

- Center for Nondestructive Characterization:
Harry E. Martz, Jr.
- Center for Precision Engineering:
Keith Carlisle

FY2002 Center Highlights

The **Center for Complex Distributed Systems (CDS)** was formed to promote technologies essential to the analysis, design, monitoring and control of large-scale, complex systems. Given the ubiquitous nature of large systems, CDS obviously covers a very broad technical area. This includes development of integrated sensing, communication and signal processing systems for efficient gathering of the data essential for real-time system monitoring. The Center also promotes the development of new methodologies for combining measured data with computer simulations in order to achieve enhanced characterization and control of complex systems. As reported in this volume, the Center has projects in information gathering, collation, and analysis. Particular emphasis is on technologies applicable to national security missions.

The **Center for Computational Engineering** orchestrates the research, development and deployment of computational technologies to aid in many facets of the Laboratory's engineering mission. Computational engineering continues to be a ubiquitous component throughout the engineering discipline. This incredible diversity requires research and development of tools that are correspondingly diverse in their breadth of application and in their depth of robust numerical treatments. The complexity and scale of emerging programmatic needs continue to drive our innovation in development and the resulting uniqueness of our fielded tools. Current activities range from tools to perform full-scale analysis of key DOE and DoD systems to design capabilities for micro-fluidic and photonic devices. Highlights of the Center's LDRD projects for this year include fundamental advances of the numerical procedures embodied in finite-element methods, adaptive methods to improve solution quality, and research to facilitate the use of the resulting simulation capabilities.

The mission of the **Center for Microtechnology** is to invent, develop, and apply microscale and nanoscale technologies to support the Laboratory missions in Stockpile Stewardship, Homeland Security, Nonproliferation, and other programs. The research topics for Microtechnology cover materials, devices, instruments, and systems that require microfabricated components, including microelectromechanical systems (MEMS), electronics, photonics, micro- and

nanostructures, and micro- and nanoactuators. This year's projects include both experimental and modeling/simulation research on: Photonics Systems, sample preparation for Pathogen Detection Systems, laser-based processes that can be used for deterministic fabrication of μm -sized features on mesoscale objects with nanoscale accuracy, and power sources for portable instrumentation and systems.

The **Center for Nondestructive Characterization (CNDC)** researches and develops nondestructive characterization measurement technology to significantly impact the manner in which the Laboratory inspects, and through this, designs and refurbishes systems and components. The Center plays a strategic and vital role in the R&D of scientific and engineering NDC technologies, such as acoustic, infrared, microwave, ultrasonic, visible and x-ray imaging, to enable Engineering in the far- to mid-term to incorporate the successful technologies into Laboratory and DOE programs. This year's LDRD projects include advancing high-spatial resolution x-ray imaging using Wölter x-ray optics; ultrasonic imaging of multilayers using arrays of transducers; research in new algorithms for ultrasonic data processing using a radial reflection diffraction tomography algorithm; and research in algorithms for

real-time microwave imaging of people through barriers such as walls and eventually to detect contraband underneath clothing.

The **Center for Precision Engineering** advances the Laboratory's high-precision capabilities in manufacturing, dimensional metrology, and assembly, to meet the future needs of the Laboratory and DOE programs. Precision engineering is a multi-disciplinary systems approach to achieve an order of magnitude greater accuracy than currently achievable. Essential to the Center's success are its core technologies, which are the building blocks for the machines, systems, and processes that will be required for future programs. The Center's core technologies are essential to the Laboratory's future because they will reduce the amount of research and development required to build the next generation of instruments and machine tools; reducing risk, design and build time, and cost. Our LDRD portfolio is driven to support this goal. Highlights for this year include the Extremely High-Bandwidth, Diamond-Tool Axis for Weapons-Physics Target Fabrication project, and our work with the other Centers on the high-accuracy x-ray imaging of mesoscale targets, as well as mesoscale deterministic fabrication.

Center for Complex Distributed Systems



Cooperative Mobile Sensing Networks

R. S. Roberts, K. A. Kent, E. D. Jones, G. H. Armstrong

Low-cost, high-endurance unmanned air vehicles (UAVs) are now practicable for autonomous sensing and data collection over wide areas. UAVs can collect data either with onboard sensors or by receiving and relaying data from ground-based sensors. Using a network of UAVs to collect sensor data would provide advantages such as quicker data collection and the ability to adapt to the loss of an individual UAV. Applications of UAV networks include providing communication services to isolated ground sensors, aerial monitoring of national borders and seaways for homeland security, and air sampling for atmospheric modeling.

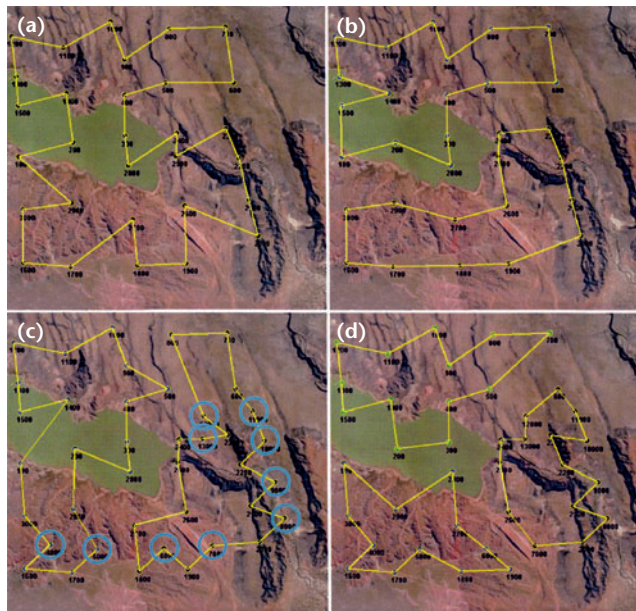
Our project investigated two fundamental requirements for using UAV networks to autonomously collect sensor data: 1) route optimization—constructing efficient routes that allow the UAVs to collect data without duplicating effort or interfering with one another; and 2) control architectures for network adaptation—allowing a network of UAVs to optimally adapt to exceptional events, such as the loss or addition of UAVs to the network or changes in the priorities of subregions in the area covered. By potentially enabling data collection by UAV, this project supports LLNL’s missions in national security and environmental management.

In FY02, we completed our investigation into UAV control architectures and network adaptation schemes, including improving our route-optimization algorithm to better process information about sensing cost—the effort required for a UAV to complete a data-collection route. Cost information is regularly estimated by each UAV and shared throughout the network. This work resulted in control architectures based on hierarchical or distributed control. In the hierarchical architectures, network adaptation is initiated by one lead UAV, which can be replaced by any other UAV should it be disabled. This type of architecture is useful in small networks requiring quick adaptation. In the distributed architectures, UAVs cooperatively perform network adaptation by individually optimizing sensing costs for their subregions. These architectures are useful in large networks in which subregion sensing costs can change abruptly—for instance, if a UAV had to remain over a specific location to video a convoy of vehicles.

In collaboration with the University of California, Davis, we continued developing a software tool called STOMP, which stands for simulation, tactical

operations, and mission planning. STOMP implements the control architectures described above to simulate, control, and communicate with UAVs used in sensing applications. The figure gives an example of network adaptability when increasing the number of UAVs and sensing points in a network. The capabilities of STOMP include simulations in which real UAVs and sensors interact with the virtual UAVs and sensors. This capability enables experiments to determine whether a sensing task requires more sensors and UAVs than are on hand.

Finally, we conducted several experiments in which an airborne UAV collected imagery from unattended ground sensors and transmitted the data to a ground station. These experiments allowed us to test the communications modules developed during FY00 and refine the data-transfer techniques developed during FY01. The results of these experiments were applied to the design of the STOMP communications objects. In summary, we developed a data-collection architecture in which UAVs collect data adaptively and cooperatively.



An example of adaptability in a network of unmanned air vehicles (UAVs) controlled with the simulation, tactical operations, and mission planning (STOMP) tool. (a) First, an area is covered by one UAV collecting data at sensing points along a route. (b) A second UAV is added, and the area is divided into two routes for faster data collection. (c) Surveillance resolution is increased by adding sensing points. (d) A third UAV is added.

Ultrawideband Communications

F. Dowla, A. Spiridon, D. Benzel, T. Rosenbury


Intelligence operations require short-range wireless communications systems capable of collecting data rapidly and transmitting it covertly and reliably. Such systems must be robust; have a low probability of detection and intercept; employ low-power, small-size hardware; and interface easily with other systems for analysis or to establish long-distance links. Commercial communication systems operate in fixed frequency bands and are easily detectable and are prone to jamming by the enemy, among other shortcomings.

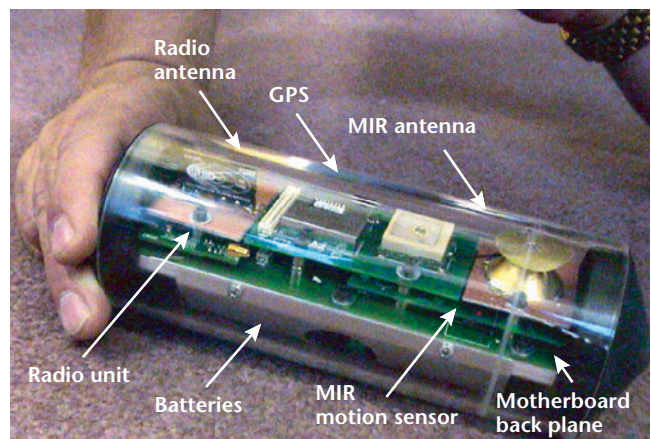
We are focusing on the three key operational modes for the Department of Defense and the intelligence community: 1) secure sensor and voice communications over a 1-km range; 2) ground-to-ground and air-to-ground data channels for small, unmanned air vehicles; and 3) network communication for large numbers of sensors in a local area, including multipath and extremely low-altitude operations.

The goal of this project is to develop and demonstrate 1) ultra-wideband (UWB) communication with a capacity of 5 Mbps and a range of 1 km; 2) multichannel capability with sensors; 3) a test bed for application development; and 4) performance standards for bit error rate and low probabilities of detection and intercept.

In FY02, we built several UWB communication transceivers for voice, video, and digital-data communications for intelligence applications (see figure). We also performed modeling and propagation analyses with multiple channels and developed 1) a UWB radio with a capacity of 2 Mbps, a range of 160 m, two channels, and a power requirement of <1 W; 2) a graphical user interface for these models; 3) an interface for real-time applications; and 4) a network and architecture design. In addition, arrays of transmitters for covert

communications were computationally modeled and simulated, and preliminary testing of the UWB communications device was conducted.

For FY03, we plan to 1) complete the modeling and propagation analysis for mobility and multipath capabilities; 2) design and implement a reconfigurable, integrated network for about ten UWB radios, including the application-layer infrastructure; 3) further refine our robust 5-Mbps, 1-km-range system to operate on <0.5 W with 10 channels, including a mobile channel; 4) develop a transmitter array for extreme covert communications; and 5) submit papers on propagation, architecture, and performance to peer-reviewed publications. 



Compact sensor node, equipped with an antenna, global positioning system (GPS), UWB radar, micropower impulse radar (MIR), processing unit, and batteries. Network protocols were developed to interface with our UWB radio design. Sensor radio nodes of this type will play a critical role in modern wireless sensor networks for intelligence and battlefield applications.

Developing Smart Seismic Arrays: A Simulation Environment, Observational Database, and Advanced Signal Processing

P. E. Harben, D. B. Harris, S. C. Myers, S. C. Larsen, K. E. Nelson

Seismic imaging and tracking methods have important potential intelligence and surveillance applications, such as tracking vehicles and detecting tunnels. However, current seismic technology cannot handle unknown geologic heterogeneity—such as variation in bedrock and soil composition—or gather and analyze data rapidly (in hours or even seconds). This project is using seismic arrays. They are capable of determining sources of continuous seismic energy and hence can be used in situations in which the distinct seismic phases cannot be associated, *i.e.*, a distinct seismic waveform feature cannot be identified by all sensor elements. These seismic arrays will be combined with an advanced data-processing system that characterizes geologic heterogeneity and allows for rapid analysis in the field, enabling applications previously thought unrealistic.

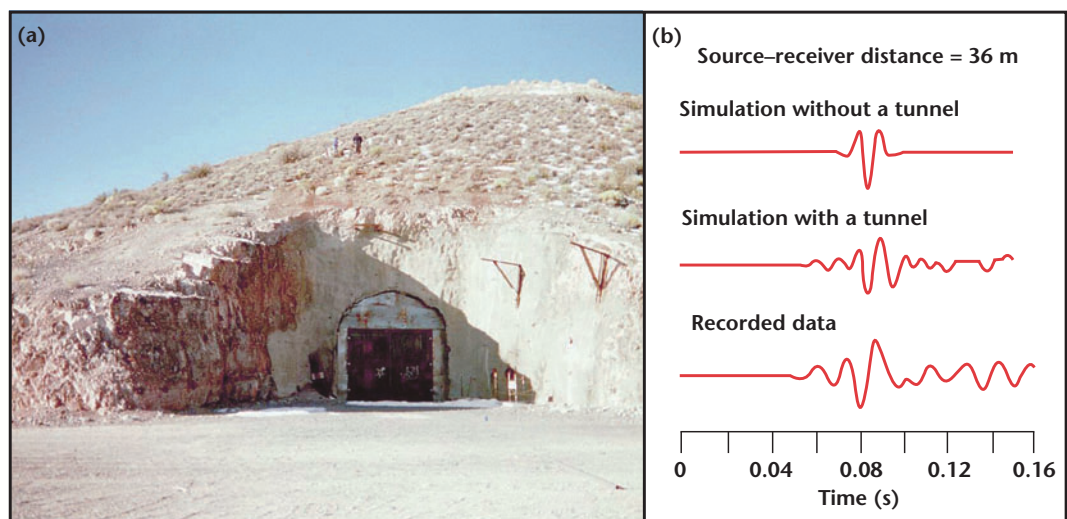
The goal of this project is to develop analysis and processing systems for seismic arrays and test the systems in tracking vehicles and imaging tunnels and other underground structures. Capabilities developed in this project will have direct application in surveillance, battlefield management, finding hard and deeply buried targets, and portal monitoring. This project thus benefits the U.S. military and intelligence community in support of LLNL's national security mission.

Detection is accomplished by determining the best fit between field data and precomputed data spanning a range of expected geologies. This strategy enables rapid analysis in the field and characterization of the influence of random geological heterogeneity. In vehicle tracking, all propagation paths to

the arrays are characterized with observed data then matched to field data to determine the best fit. In underground imaging, LLNL's total wave field modeling code—E3D—is run for all expected tunnel configurations and expected geological heterogeneity, which are then matched to the field data for a best fit.

In FY02, we tested the data-processing strategy for vehicle tracking. At a test site at LLNL, three seismic arrays were to track a tank in real time. The results demonstrated that with three seismic arrays, a tank could be tracked from as far as a few miles away. This aspect of the project will be spun off in FY03 and supported by the Department of Defense. We also used the data-processing system in imaging underground structures at the Nevada Test Site. The results, shown in the figure, demonstrate that our methodology has promise in tunnel detection. Near the end of the fiscal year, much more extensive testing was conducted at a mine safety laboratory in Lake Lynn, Pennsylvania, to attempt detection of a deeper tunnel in a more realistic and difficult environment. Results will be available in FY03.

In FY03 we will test our data-analysis methodology by generating data with E3D for a large number of geological realizations and matching the E3D data with field data from the Lake Lynn site. Other objectives include analysis of past data from tunnel explosions at Lake Lynn to determine whether our seismic arrays and data-processing methodology can determine the origins of simultaneous, noncoincident ordnance detonations.



Seismic arrays and data-processing technology tested at the Nevada Test Site. (a) The tunnel over which field data was recorded. (b) Results of E3D simulations conducted with and without a tunnel. The model simulation with a tunnel best agrees with the field data, demonstrating the effectiveness of our seismic-array system.

Infrastructure Response to Natural and Man-Made Ground Motions: High-Performance Computing and Distributed Sensing for Regional Scale Prediction and Response

D. B. McCallen, S. C. Larsen, A. J. Rodgers


Earthquakes and underground nuclear explosions disperse tremendous energy into geologic strata. This energy propagates large distances in the form of traveling seismic waves, which shake the ground surface and can present a serious hazard to man-made structures. Measurements of earthquake- and nuclear-test-generated ground motions have indicated that the strength of these motions varies greatly with spatial location. Shaking intensity at any site is a complex function of the energy source mechanism, the geologic path along which the seismic waves propagate, and the soil conditions below the site. Also, the direct relationship between the vibrational characteristics of a particular structure and the frequency content of the ground motion will control the degree to which a particular structure is shaken. Until recently, scientists and engineers have relied on relatively simple empirical relationships to estimate the motions to which a structure might be subjected. However, this approach often requires generalization and extrapolation from the existing knowledge base and is limited because of the complexities of wave propagation in the heterogeneous earth. While such approaches might be adequate for basic structure design information (e.g., sizing members, estimating structural deformations), they do not provide detailed information on the response levels that can be expected for a specific earthquake that might occur.

With the advent of massively parallel computers, it has become feasible to simulate the physics of energy propagation from the source through the earth and into a structure. Such an approach makes it possible to generate more realistic site-specific motions that account for the propagation path, local soil response, and interaction between the seismic waves and the structure. In the current study, a regional combined geophysics-structural model is under development. The Southern Nevada region encompassing the Las Vegas Valley and the Nevada Test Site (NTS) (see figure) is serving as a case study for the model development. In addition to providing a regional model of unprecedented scope and extent, the research results will provide a tool to enable the NNSA to assess nuclear test readiness and understand the seismic hazard to the rapidly growing Las Vegas Valley in the event the nation must resume testing. In addition to supporting this national security mission, the research will spin off the tools and knowledge necessary to predict earthquake hazards and enhance safety in earthquake-prone areas.

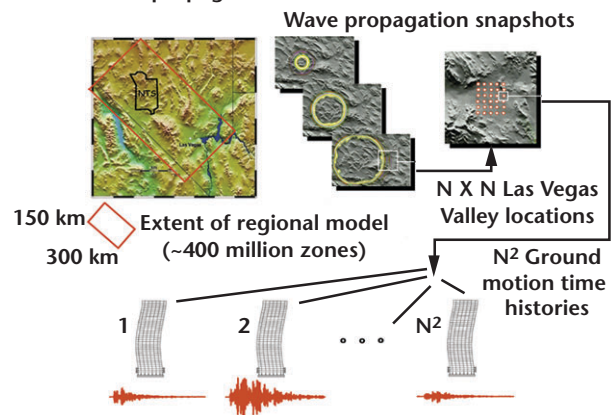
The regional model framework is called NEVADA and includes a finite-difference wave-propagation code coupled to a special-purpose structural finite-element

program that permits linear and nonlinear analysis of building systems. Once a source function at NTS is defined, the regional model propagates seismic energy into the Las Vegas Valley and analyzes the response of a specified structure at preselected locations throughout the valley. This simulation essentially provides a regional seismic hazard assessment with a single program execution.

In FY02, we successfully developed the geophysics model of the Southern Nevada region, created the special structural modeling code, and coupled the codes on Livermore's Advanced Simulation and Computing (ASCI)-level compute engines. We demonstrated the practicality of this coupled regional simulation with actual source-to-structure simulations on the ASCI Blue computer. Our geology characterization was completed in close collaboration with University of Nevada researchers. Parametric simulations with the regional model indicate dramatic variations of ground motion and structural response across the Las Vegas Valley as a result of basin amplification effects. This correlates with the legacy measured nuclear test data, which indicates ground motion amplitude variations by factors as great as 10 to 20 across the Las Vegas Valley.

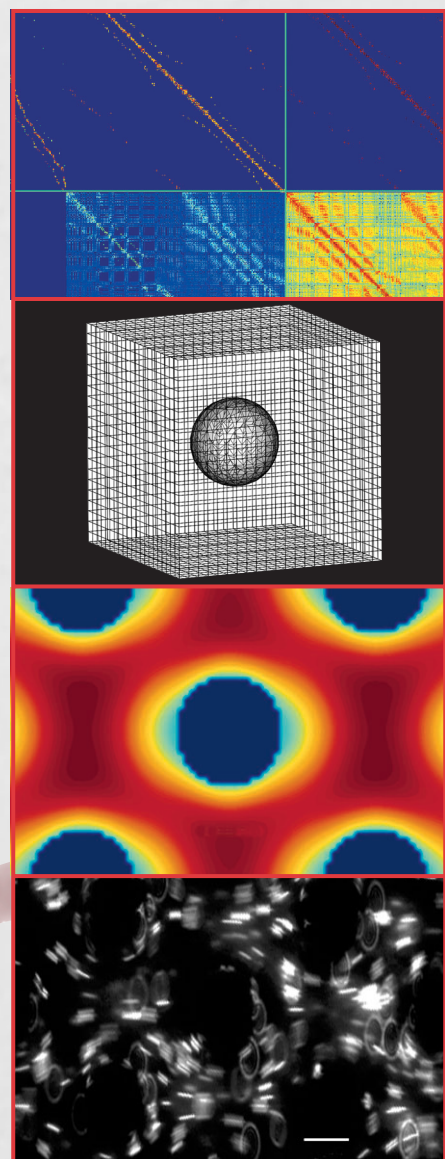
In FY03 we intend to complete additional parametric studies of regional response to determine the degree to which observed ground motion variabilities are controlled by basin topography or by local soil site response. These parametric studies will also validate the simulation models by comparison with actual ground motion data. The NEVADA framework will be ultimately handed off to program staff to undertake programmatic applications with the software. 

Seismic wave propagation simulation:



A geophysical model of the Southern Nevada region that encompasses the Las Vegas Valley and the Nevada Test Site, combined with a structural model and used to simulate the propagation of seismic energy from the ground to the structure.

Center for Computational Engineering



Numerical Technology for Large-Scale Computational Electromagnetics

R. M. Sharpe, D. A. White, N. J. Champagne, M. Stowell


The key bottleneck of implicit computational electromagnetics (CEM) tools for large complex, geometries—such as those addressed in the Advanced Simulation and Computing (ASCI) program—is the solution of the resulting linear system of equations. The goal of this effort is to research and develop critical numerical technology that alleviates this bottleneck for large-scale CEM by greatly reducing the time required to solve the associated hybrid linear systems of equations.

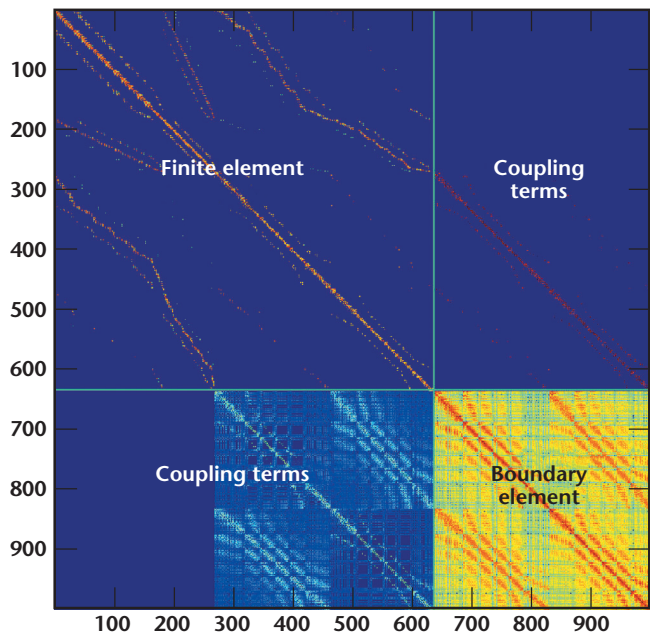
The mathematical operators and numerical formulations used in this arena of CEM yield linear equations that are complex valued, unstructured, and indefinite. In addition, simultaneously applying multiple mathematical modeling formulations to different portions of a complex problem (hybrid formulations) results in a mixed-structure linear system, further increasing the computational difficulty. Typically, these hybrid linear systems are solved using a direct solution method, which was acceptable for Cray-class machines but does not scale adequately for ASCI-class machines. In addition, LLNL's existing linear solvers are not well suited for the linear systems that are created by hybrid implicit CEM codes.

Activities in previous years of this project focused on establishing a test suite of sample matrices to evaluate the solver research; extending the ISIS++ solver framework to treat complex-valued, hybrid linear systems by supplementing the native iterative methods in the package with several direct solvers; and implementing a Shur-complement approach for solving block-structured hybrid linear systems. We also identified the need for both matrix- and operator-based preconditioners. Matrix-based methods can be applied to any linear system of equations after the matrix has been assembled.

In FY02, work on sparse approximate inverse preconditioners and on incomplete lower/upper preconditioners was completed and incorporated into the final solver package. Research on direct operator-based methods, initially performed with R. J. Adams of the University of Kentucky, recast integral equations of the

first kind into integral equations of the second kind. Preliminary results indicate improvement in the basic conditioning of the linear system that reduces solution time by two orders of magnitude for some systems of equations. The figure is an example of a hybrid matrix for a coupled finite element–boundary element solution of Maxwell's equations.

Previous work on a single-level multipole algorithm—a method shown to reduce the operation count from N^2 to $N \log(N)$ for linear systems to which they apply—was extended to a multilevel algorithm, which further improved the solution performance and increased computational speed. All of the results from this LDRD project are being incorporated into LLNL's solver framework for researchers involved in CEM. 



Example of a hybrid matrix for a coupled finite element–boundary element solution of Maxwell's equations. Blue represents zero matrix values. The finite element represents a discretization of the Helmholtz equation, and the boundary element represents a discretization of the electric-field integral equation.

Generalized Methods for Finite-Element Interfaces

M. A. Puso, E. Zywicz

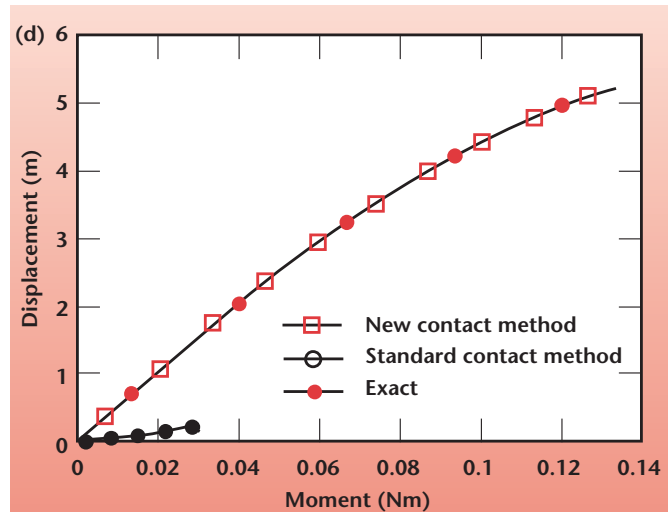
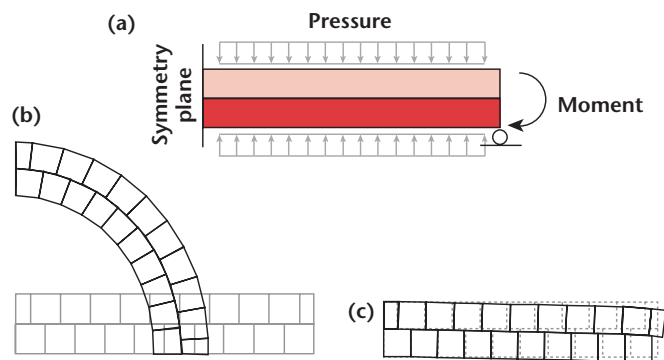
With the increasing complexity of finite-element models, it has become essential to mesh individual parts of a finite-element model independently such that nodes at part boundaries are not aligned. Current finite-element techniques for connecting (*i.e.*, gluing, tying) these dissimilar meshes together at the boundary often cause serious errors in a stress analysis. Aware of this fact, engineering analysts work to avoid dissimilar meshes—often to no avail. Furthermore, the trend for teams of analysts to work independently on different weapons subassemblies makes the need for accurate dissimilar-mesh connection more acute.

The goal of this project is to solve the problem of connecting dissimilar meshes through research in accurate numerical methods that will eliminate the need to produce conforming meshes. If successful, this new technology can potentially save vast amounts of time and money across the DOE Complex. For example, a large weapons model often takes a month to build, and will undergo many revisions over a matter of years. Analysts estimate that a method for connecting dissimilar meshes may save up to 25% of their time in meshing over the course of a project, without sacrificing accuracy. In addition, similar numerical problems occur when interfacing meshes slide with contact. Our new mortar method techniques are now being applied to improve contact-surface modeling. This project enhances LLNL's competency in computational mechanics in support of stockpile stewardship.

The “mortar method” for connecting two-dimensional (2-D), flat interfaces has been extended to connect arbitrary 3-D, curved meshes so that optimal convergence is achieved. In this way, refinement of the dissimilar mesh will have the same asymptotic convergence rate as the conforming mesh—dissimilar meshing will not compromise mesh quality. This method requires solving surface integrals involving Lagrange multiplier fields for traction and displacement. Such surface integrals are straightforward for 2-D, flat interfaces but complicated for 3-D, curved surfaces. In FY01, we developed a closest-point projection-type algorithm for 3-D surface integrals and used simple Lagrange multiplier fields to demonstrate optimal convergence on 3-D models with curved, tied interfaces.

In FY02, we further developed our theory for stability conditions; implemented a dual formulation for the Lagrange multiplier fields, which sped calculation times by a factor of 7 over our previous results; and began work on the mortar method for contact. Mortar contact resolves the mortar-averaged gap function into normal penetration and frictional slip, provides vastly superior convergence behavior, and eliminates the locking associated with the standard contact methods in high-pressure environments, as seen in the figure.

In FY03, we plan to finish mortar normal contact, incorporate friction into contact simulations, and apply our methods to discretizations involving higher-order elements.



Our “mortar method.” (a) Contacting beams with ambient pressure and applied moment. (b) Resulting deformation using new mortar contact. (c) Pathological locking behavior demonstrated by standard contact. (d) Simulated results versus analytically exact solution.

Higher-Order, Mixed Finite-Element Methods for Time-Domain Electromagnetics

N. K. Madsen, D. A. White, N. J. Champagne


Time-domain computational electromagnetic (CEM) modeling is the most cost-effective approach for electromagnetic design and analysis for problems that are electromagnetically very large or nonlinear and transient in nature. However, no stable, higher-order, conservative methods—such as those that exist for computational fluid dynamics and other disciplines—exist for time-domain CEM, largely because of the unique characteristics possessed by Maxwell’s equations, which are typically solved with a set of low-order, Cartesian-grid methods. These simple, stable methods work well for rectangular geometries but require prohibitively large meshes for quantitative field predictions on electrically large problems and produce inconsistent solutions for nonorthogonal geometries. In addition, finite-volume schemes, which are often considered as an alternative, suffer from numerical instabilities, lack of conservation, and low accuracy.

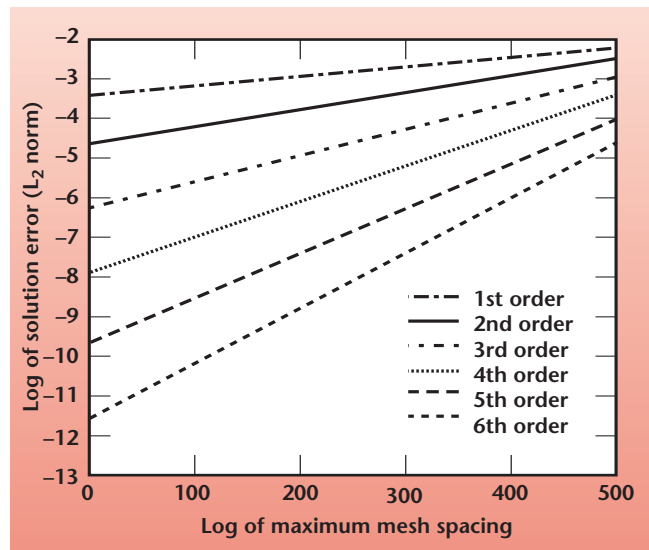
To overcome these limitations, this project is investigating higher-order, mixed finite-element methods (MFEM)—a new methodology for solving partial differential equations on three-dimensional (3-D), unstructured grids. Our goal is to develop a stable, conservative, higher-order, and accurate simulation code for Maxwell’s equations and related equations of electromagnetism. Our MFEM methodology builds on LLNL’s competency in computational engineering and will 1) enable engineers to perform electromagnetic simulations on unstructured grids, and 2) provide a coupled electrothermalmechanical modeling capability, both in support of the Laboratory’s national security mission.

Accomplishments in FY02 include 1) making progress on the core higher-order numerical components of our simulation code, such as integration rules, basis functions, and the hexahedron, tetrahedron, and prism elements; 2) collaborating with a consulting firm to develop software components for assembling and solving, in parallel, the global linear systems; and 3) using these software components to demonstrate the efficacy of higher-order methods and perform a time-dependent simulation using higher-order time-integration methods.

To demonstrate accuracy, we used MFEM methods of various orders to solve the vector Helmholtz equation

for a resonator. The figure shows the rate of error decreasing as the mesh spacing is refined. The sixth-order method achieves, for the first time at LLNL, almost 12 digits of solution accuracy. We also studied using adaptive Runge-Kutta schemes for time-dependent problems and tested our high-order basis functions in the parallel assembly of mass and stiffness matrices for arbitrary-order, finite-element discretization.

Our work in FY03 will focus on 1) completing our prototype parallel, higher-order electromagnetic-application code; 2) further evaluating this code by comparing computed results to well-known solutions; 3) preparing and submitting journal articles about our underlying numerical methods; 4) modifying our software to improve parallel efficiency, scalability, and ease-of-use; and 5) demonstrating our technology by simulating important, longstanding issues in CEM—such as absorbing boundary conditions, mesh refinement, and material models—that existing methodologies cannot effectively simulate. 



MFEM methods of various orders to solve the vector Helmholtz equation for a resonator. The figure shows that the rate of error decreases as mesh spacing is refined, and that the sixth-order method achieves almost 12 digits of solution accuracy.

Exploratory Research into the Extended Finite-Element Method

R. M. Sharpe, K. D. Mish

The finite-element method has become the standard tool of computational mechanics in the national laboratory community. This simulation tool accounts for the vast majority of computational analyses performed in support of LLNL's engineering work; and general-purpose finite-element LLNL physics codes such as DYNA3D and ALE3D represent the pinnacle of simulation-based practice in mechanical engineering.

Unfortunately, conventional unstructured finite-element applications are optimized for designing idealized mechanical systems, whereas LLNL missions such as stockpile stewardship are more concerned with analysis of as-built systems. Tools optimized for general mechanical design can, with sufficient effort, provide efficient mechanical analysis of as-built systems. However, discrepancies between idealized and as-built mechanical configurations may be considerable and may, in fact, render analyses based on idealized configurations woefully inadequate.


The goal of this project is to develop extended finite-element (XFEM) techniques by improving conventional finite-element modeling so that the actual configuration of as-built mechanical systems can be subjected to a broader range of mechanics simulations. This XFEM technology will remedy some of the most onerous limitations of finite-element modeling relevant to LLNL needs, such as localization and singular response near cracks and imperfections. This project will substantially

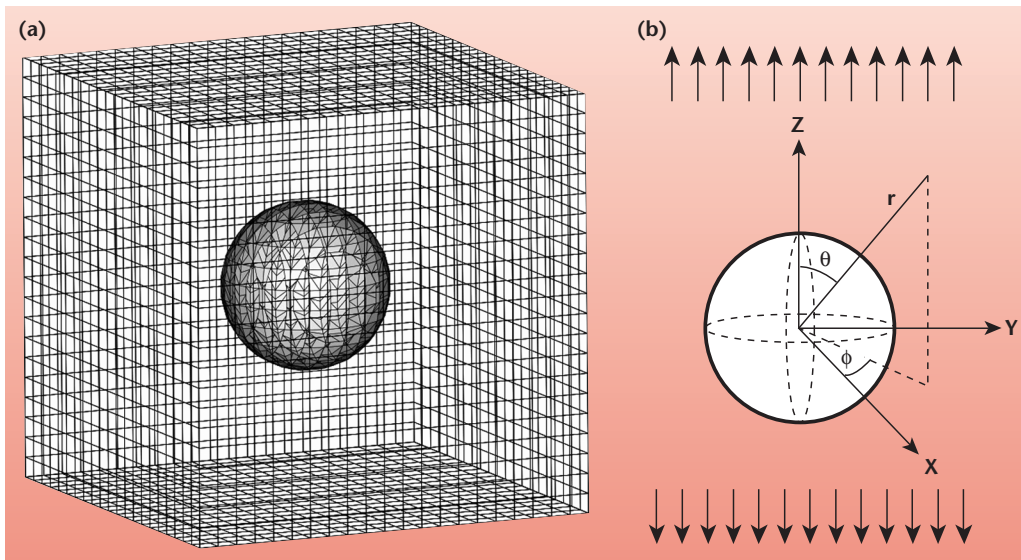
extend LLNL's core competence in computational science and engineering and its capabilities in nuclear weapons engineering and manufacturing technologies in support of DOE's national security mission.

During FY02, applied mechanics results achieved in FY01 in the area of crack propagation and material interface were extended to integrate XFEM techniques into computer-aided engineering. In particular, additional capabilities essential for computer-aided problem setup goals—such as automation of mesh generation and material identification—were explored and demonstrated.

Several promising new techniques developed to automate the analysis process include 1) radial basis functions—a new technique for implicit surface definition originally developed for computer graphics rendering—for determining the boundaries of a mechanical system; 2) improved integration techniques for evaluating the governing XFEM equations over regions with irregular material boundaries, cracks, or contact surfaces; and 3) new enrichment functions for modeling voids and other localization phenomena commonly found in materials used in weapons engineering.

Validation of the XFEM techniques included using these new methods to analyze problems with closed-form solutions so that convergence rates can be studied. Figure (a) shows a typical validation problem, in which a spherical inclusion is modeled in an otherwise uniform and isotropic body—represented with a structured

XFEM mesh—subjected to uniaxial tension. Figure (b) is the model's boundary-value problem description. Convergence tests demonstrate that both structured and unstructured XFEM solutions converge at the same rate as conventional finite-element methods, which means that these XFEM techniques can be used to construct meshes for analysis with less effort but without compromising accuracy. 



Validation of extended finite-element (XFEM) simulation techniques intended to extend the applicability of the finite-element method to as-built mechanical simulations. (a) A spherical inclusion modeled in an otherwise uniform and isotropic body—represented with a structured XFEM mesh—subjected to uniaxial tension. (b) The model's boundary-value problem description, in which arrows indicate the direction of tension.

Modeling and Characterization of Recompressed Damaged Materials

R. Becker


Ductile metals subjected to shock loading can develop internal damage through nucleation growth and coalescence of voids. The extent of damage can range from a well-defined spall plane induced by light shocks to more widespread damage caused by strong shocks. Because damaged materials are often part of a dynamic system, significant additional deformation and recompression can occur in the damaged region. To represent material behavior correctly in simulation codes for applications such as stockpile stewardship calculations, both the damage and the recompression processes must be modeled accurately. Currently, no experimentally based models of recompression behavior are available for use in numerical simulations.

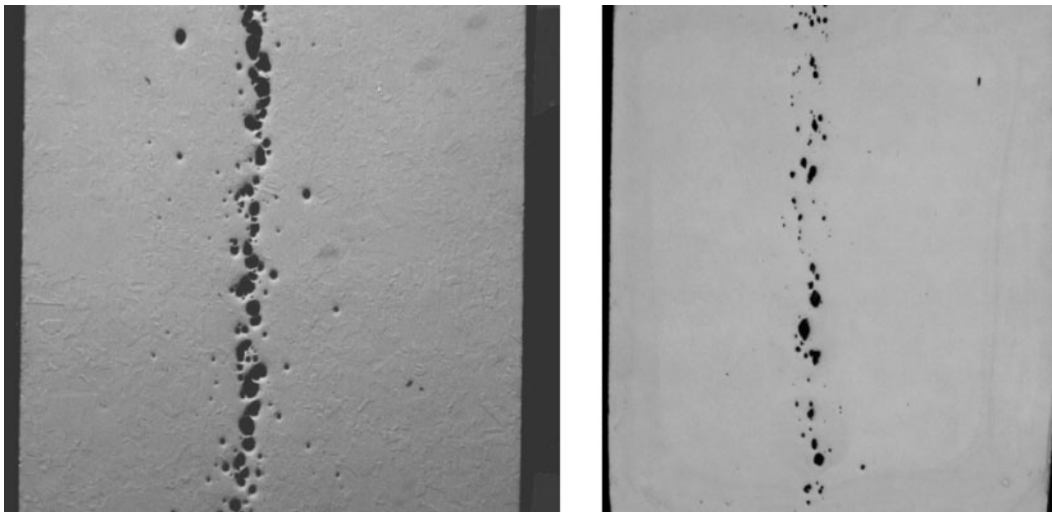
The goals of this project are to 1) perform recompression experiments on samples containing controlled and well-characterized damage, 2) develop a model that captures the recompression behavior and residual strength based on the experimental data and micromechanical models, and 3) implement the model in the Advanced Simulation and Computing (ASCI) code ALE3D. The recompression model, together with failure models based on underlying physical mechanisms, will provide a more accurate representation of the behavior of explosively loaded materials. Accurate modeling of the deformation of severely damaged materials is important for stockpile stewardship simulations and DoD applications.

The experiments involve creating a controlled level of damage inside material specimens in the form of spall-induced porosity. The material is then compressed to close the porosity and subsequently tested to determine the strength of the recompressed material.

Samples are taken from each stage of the process to observe the damage level through standard metallographic techniques. For the experiments conducted in FY02, the spall damage was introduced in the copper specimens through impact experiments conducted on a light gas gun. The damaged material was recovered and compressed 15% at quasistatic strain rates and in a split Hopkinson bar at dynamic strain rates of 3000/s. Following recompression, tensile specimens were machined and tested to assess the residual strength of the material.

The strength of the damaged region during compression was unexpectedly high. Although the spall-related porosity accounted for a significant fraction of the total area on the spall plane, the strength of the damaged region in compression was high enough to resist deformation while the surrounding material deformed. A large fraction of the 15% compressive deformation occurred outside the damaged region. Our results indicate that this is due to the significant strain hardening of the highly-strained material surrounding the voids.

Additional experimental and simulation work is planned for FY03 to better define and characterize the material response during recompression. Simulations will be used to determine the role of strain hardening on the void closure behavior. Recompression experiments will be pursued using higher pressures available with a gas gun and lasers. The laser experiments are particularly interesting since they access a much higher pressure and strain-rate regime. The additional data will provide more confidence in the model when it is applied to simulating materials under extreme conditions. 



Spall damage in copper specimen (left) before and (right) after 15% compression. Significant compression has occurred outside the damaged region.

Dynamic Simulation Tools for the Analysis and Optimization of Novel Filtration, Sample Collection, and Preparation Systems

D. S. Clague, T. H. Weisgraber, K. D. Ness

Heighted attention on chemical and biological early-detection systems has increased the need for high-efficiency filtration, collection, and sample-preparation systems. To study and understand the physics governing such systems, optimize these critical operations, and characterize system efficiencies based on the details of the microstructure and environmental (temperature) effects, we will develop advanced computational analysis tools—new lattice Boltzmann (LB) simulation capabilities for studying fluid behavior not by tracking individual fluid molecules, but by tracking a probability-distribution function that represents the collective behavior of fluid molecules in local regions. This new simulation capability will be validated with experimental data.


These new simulation tools will have a direct impact on filtration, collection, and sample-preparation systems that support the Laboratory's chemical and biological counter-proliferation and homeland security missions.

In FY02, we developed an input module for ordered arrays of cylinders to replicate the microstructure of a novel DNA purification device, the pillar chip. This device, in which DNA is preferentially trapped on the pillar surfaces, has received wide acceptance here at LLNL. Design and analysis tools to optimize chip performance are therefore crucial.

Initial LB simulations were performed to analyze velocity and shear stress through different pillar

arrangements with various cross sections. The goal is to maximize the available surface area for capture by characterizing fluid velocity and shear stress at pillar surfaces for various proposed designs. An example velocity field is shown in Fig. 1 for a periodic pillar array in a 50-mm-deep channel. The Reynolds number based on the 8-mm-diam pillars was 0.026. Both velocity and shear stress exhibited strong gradients due to the close packing of the cylinders, which will strongly influence species transport and capture in the device.

To validate the LB capability, digital particle image velocimetry experiments were conducted to measure the velocity profile through the pillars (Fig. 2). We also developed theory to incorporate electrostatic and van der Waals interactions between suspended species and pillars; these colloidal interactions were incorporated into the LB method. These new capabilities are directly relevant to ongoing research efforts that use the pillar chip.

In FY03, we will develop 1) a generalized porous media generation module that includes pillar geometries, porous membranes and fibrous filters; 2) colloidal interaction theory specific to porous membranes; 3) a novel approach to incorporate Brownian motion; 4) a coupled-energy equation to account for environmental effects; and 5) a characterization of species transport properties through, and capture efficiencies in, a pillar chip with and without environmental effects. 

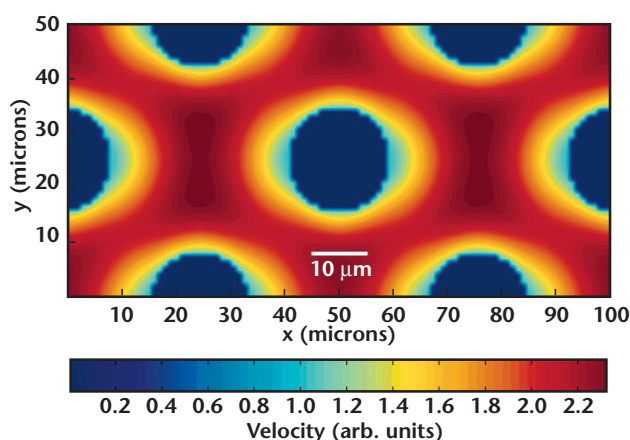


Figure 1. Lattice Boltzmann simulation of fluid velocity through a pillar array.

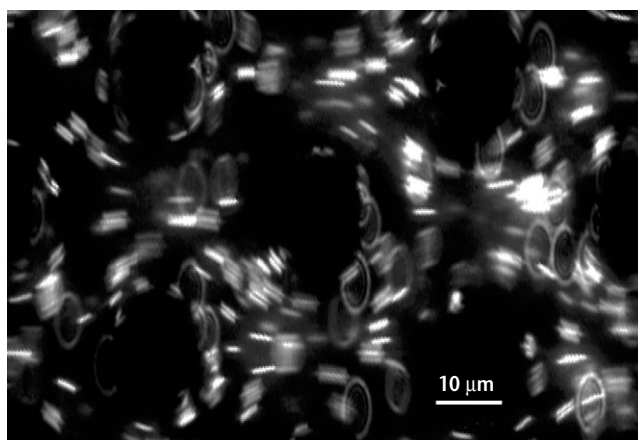
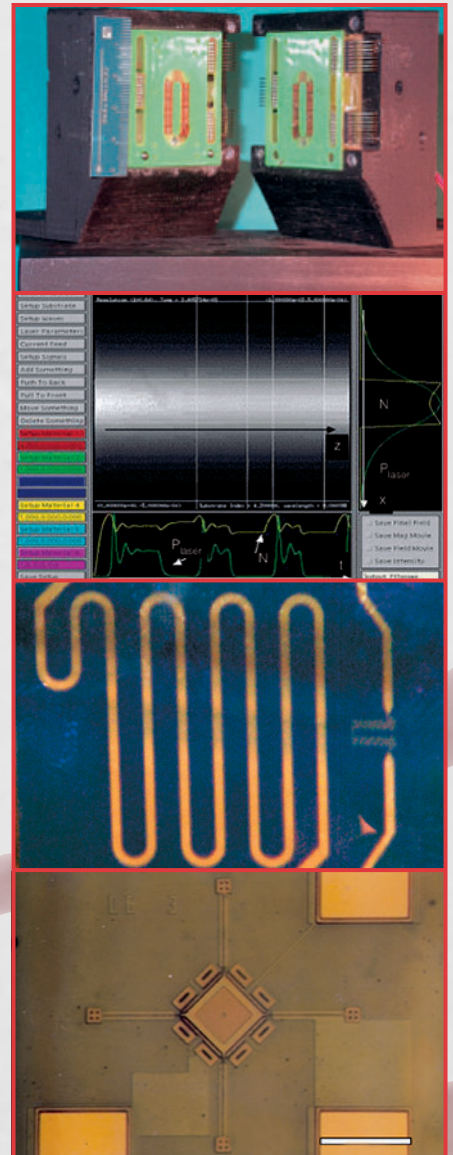


Figure 2. Experimental image of particles flowing through the pillar array.

Center for Microtechnology



Reconfigurable, Optical Code-Division Multiple Access for Fiber-Optic Networks

S. W. Bond, R. J. Welty, I. Y. Han, C. V. Bennett, E. M. Behymer, V. R. Sperry, S. J. Yoo

High-speed, high-capacity fiber-optic communications networks, which allow multiple users to access the same network simultaneously by sharing the same transmission medium, have proliferated for long-distance, metropolitan, and local-area communications systems. Recently, a rapid expansion has begun into wavelength division multiplexing (WDM) systems, which use multiple wavelengths to increase capacity. In addition, code-division multiple-access (CDMA) techniques, which were originally developed for wireless communications, can also be used to further increase the number of channels on an optical fiber.


This project entails the development of advanced technologies that have potential applications to national security—such as secure, high-speed transmissions—and that will enhance LLNL's competencies in optoelectronics and high-speed communications.

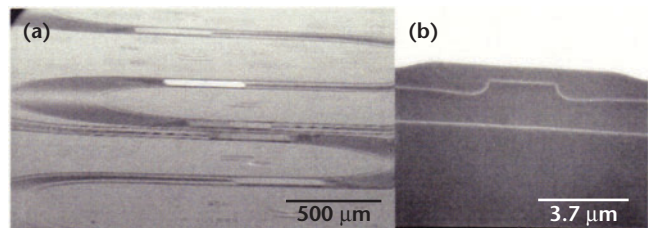
By applying innovations in WDM-component technology, we are developing a compact optical CDMA (O-CDMA) encoding and decoding device that would handle large code sizes, be remotely reconfigurable by a network operator, and be compatible with commercial fiber-optic infrastructures. The device, which comprises two indium phosphide (InP) arrayed waveguide gratings (AWG) and an array of InP phase modulators, would allow each user of a network to spectrally phase-modulate (encode) a broadband, ultrashort, transmitted optical pulse. Only the intended recipient, in possession of the correct complementary phase code, would be able to decode the transmitted information. The use of InP enables single-chip integration of active and passive components for operation at telecommunication wavelengths of ~ 1550 nm, which is not possible with other semiconductor materials.

Our approach uses broadband, ultrafast (300-fs) pulses from an actively mode-locked, erbium-doped, fiber-ring laser operating at $1.55 \mu\text{m}$ with a 2.488-GHz

repetition rate, which is equivalent to a SONET OC-48 rate. These pulses are spectrally phase-encoded by transmitting them through the monolithically integrated semiconductor device. In this process, the input AWG, functioning as a diffraction grating, spectrally slices the input pulse. Next, the spectral components are phase delayed by an electrically controlled waveguide phase modulator and then recombined by the output AWG for insertion into the network. This device allows a network operator or user to change the transmitted or received code at very high speeds by phase-trimming each spectral slice of the optical pulse.

In FY02, we 1) utilized the waveguide and device designs made in FY01 to grow InP material for the AWGs using metal-organic chemical vapor deposition (see figure); 2) demonstrated wet-etched fabrication of an AWG device [Fig. (a)]; 3) developed InP regrowth techniques for creating an upper cladding material for some waveguide designs [Fig. (b)]; and 4) installed an electron cyclotron resonance (ECR) dry-etching facility for improved curved waveguide fabrication.

In FY03, we plan to complete fabrication of the InP-based integrated device using the ECR dry-etching facility and to demonstrate spectral phase coding of a 300-fs optical broadband pulse. 



Scanning electron microscope photographs of indium phosphide (InP) components fabricated for a compact optical code-division multiple-access device. (a) An arrayed waveguide grating created by wet-etching InP material grown by metal-organic chemical vapor deposition (MOCVD). (b) InP top cladding material regrown on a rib waveguide using MOCVD.

Modeling Tools Development for the Analysis and Design of Photonic Integrated Circuits

T. C. Bond, J. K. Kallman, G. H. Khanaka

Photonic integrated circuits (PICs), which use light (photons) rather than electricity to process information, are predicted to be the next generation of high-speed processing chips. Recent advancements in material processing and device engineering are leading to integration of various optical components on a single chip. Such an optical chip could potentially enable highly compact, low-latency, wide-bandwidth, ultrafast, secure information systems. PIC design tools are needed to advance all-optical logic systems for data transmission and signal processing by reducing development time and cost, but commercial software is limited to a restricted suite of problems. The goal of this project is to create sophisticated PIC simulation tools that will benefit LLNL missions in national security, including stockpile stewardship, weapons miniaturization, high-bandwidth diagnostics, remote sensing, high-performance computing, and secure communications.

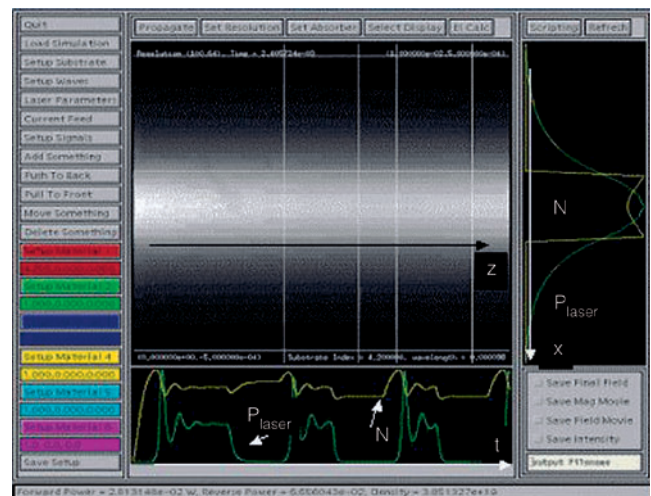
We focused on novel lasers and nonlinear devices—such as logic gates—for all-optical digital circuits and signal processing, and highly sensitive sensors for analog and digital operations. For instance, the Boolean logic on which computer technology is based can be realized in PICs by integrating laser gain elements with dielectric waveguides as both optical inputs and outputs.

In FY02, we generated frequency-domain (FD) and time-domain (TD) codes for the analysis and design, respectively, of laser-based digital gates in their steady and dynamic states. Both one-dimensional (1-D) and 2-D codes were developed using several methodologies, e.g., the Runge-Kutta and Brent's methods, finite-difference TD, and the beam propagation method tool. The codes—written in Java or C++, validated against existing data, and provided with a graphical user interface (GUI)—were used to accurately investigate the effects of gain leverage, gain quench, and other critical physical effects on gate efficiency for a wide range of geometries and material parameters, such as applied current, length, and mirrors reflectivities. The 1-D models are capable of treating wavelength dependence of the gain and spectral hole burning; they were used to analyze simple standard lasers and to benchmark the 2-D codes. The 2-D codes allow multi-mode structures analysis, are inherently scalable to a vectorial formulation, and include carrier diffusion,

which is critical for analyzing spatial hole burning and gain guiding.

The figure is a 2-D TD simulation of a NOR operation in a three-section, optically controlled, Fabry-Perot edge-emitting gallium-arsenide multi-quantum well laser. This and other simulations indicate that higher gain (fan-out) and deeper modulation depth (signal restoration) are obtained with longer control regions and wider lasers operating close to threshold, and that operating frequencies (clock rate) up to a few GHz could be achieved at the expense of the applied current, above which switching is possible but level restoration is insufficient.

Goals for FY03 are to complete, package, and deliver the suite of 2-D models for designing PICs. These steps include thoroughly checking consistency among the codes, fine-tuning the GUI to improve ease of use, and writing documentation. In addition, the need and feasibility of 3-D tools for the analysis of inherently complex full 3-D structures will be investigated.



Screen capture of the two-dimensional time-domain code simulating the Boolean NOR operation for analyzing and designing photonic integrated circuits. First one control is on, then two controls are on (deeper valleys). Central window: longitudinal distribution of photons (white) at a chosen time, showing the effect of gain-guiding. Side window: Cross-sectional distribution of power (green) and carrier density (yellow), demonstrating diffusion of the carrier. Bottom window: time distribution of power and carrier density. When two controls are on, modulation is deeper and faster as expected.

Disposable Polymerase Chain Reaction Device

E. K. Wheeler, W. Benett, K. D. Ness, P. Stratton, A. Chen, A. Christian, J. Richards, T. H. Weisgraber

The September 11, 2001 attack on the United States and the subsequent anthrax scare have raised antiterrorist vigilance to new heights. Although the September 11 attack was orchestrated with hijacked planes, the next threat could be nuclear, chemical, or—as evidenced by the anthrax scare—biological. Many countries that may support terrorist activities are likely to have biological weapons capabilities; biological weapons are probably also available on the black market and accessible to domestic terrorists. Planning and equipping for a biological attack requires detection devices that are robust in the field, easy to use, and relatively inexpensive. This project will leverage LLNL's competencies in microtechnology and instrumentation and will provide new capabilities in support of LLNL's homeland security mission.

To take appropriate action, first responders to a biological attack (local emergency response personnel, military, or intelligence personnel) must identify the specific organism used in the release. For this purpose, polymerase chain reaction (PCR) assays are becoming increasingly important because they can amplify a target segment of DNA (by thermal cycling of the necessary reagents) and enable identification of pathogens. However, the sophisticated tools needed to assess a potential biological release not only are unaffordable to many first-response agencies, but also require highly trained individuals.

In this project, we are designing and demonstrating a compact, disposable PCR unit based on a novel thermal cycler. The PCR device will allow first responders at the scene of a biological attack to quickly identify the nature and extent of the attack. By building on LLNL's success in designing portable PCR units, we are seeking to develop low-cost, disposable PCR units to be used by first responders. Authorities looking for

the source of contamination in food or water will also benefit from this device.


During FY02 we focused on improving and testing our novel convective PCR thermal cycler, which uses the thermal convective forces created by fixed, nonfluctuating, hotter- and cooler-temperature regions to thermally cycle the sample fluid to achieve amplification. The advantage of this approach is lower power requirements, increasing the probability that small batteries will suffice as the system's power source. We used our thermal cycler to successfully amplify a 90-base-pair, multiple-cloning site segment of a DNA plasmid—one of the first times DNA amplification has been accomplished using convective forces.

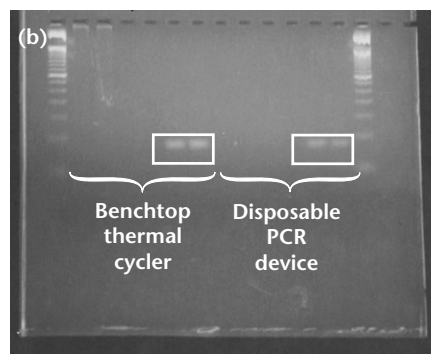
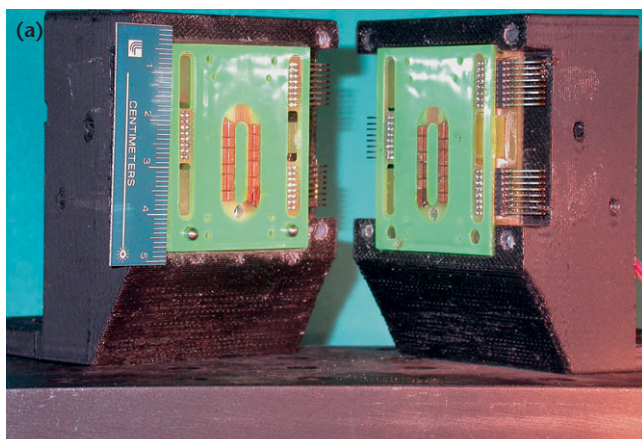
Successful DNA amplification requires an optimum temperature profile in the thermal cycler—for example, its heaters must not produce local hot spots. We fabricated several types of heating systems and achieved one that satisfied this and other thermal requirements; a patent application was filed for this heating scheme.

Sample fluid velocity was also addressed. Because the DNA amplicon—the amplified segment of DNA—in a sample fluid doubles each time the fluid cycles through the PCR unit, greater fluid velocity reduces the time needed for detectable amplification, further lowering power requirements. Measurements made with digital particle image velocimetry during test cycling yielded a fluid velocity of 1.6 to 2.4 mm/s—in excellent agreement with the velocity (2.8 mm/s) predicted as necessary with models in FY01.

In addition, we began designing a sample-preparation system based on a pillar chip—a device that captures DNA on silica pillars while inhibitors are removed, after which a series of wash steps releases the DNA from the pillars for thermal amplification.

In FY03, we will continue thermal optimization of the

cycler and begin work to incorporate sample preparation with the thermal cycler—crucial for an integrated, easy-to-use, low-power, robust, and disposable PCR device. 



(a) The convectively driven polymerase chain reaction (PCR) thermal cycler developed in this project. (b) Gel detection showing successful amplification of a 90-base-pair, multiple-cloning-site segment of plasmid DNA using our device, compared to amplification with a standard benchtop thermal cycler.

Integrated Microfluidic Fuel Processor for Miniature Power Sources

R. S. Upadhye, J. D. Morse, A. F. Jankowski, M. A. Havstad


Improving portable power sources is a critical issue for the military, weapons-testing monitors, and the intelligence community. Commercially available batteries are inadequate for advanced applications in remote reconnaissance, intelligence gathering, and telemetry. Such applications require lighter-weight, longer-lasting power sources meeting specific performance criteria. Current proton-exchange (PEM) fuel cells are limited to 3 to 15% methanol solution, which restricts power and energy density. We are developing a PEM fuel cell with a separate microreactor that converts the methanol to hydrogen, thus exploiting the very high energy densities of methanol and other liquid fuels.

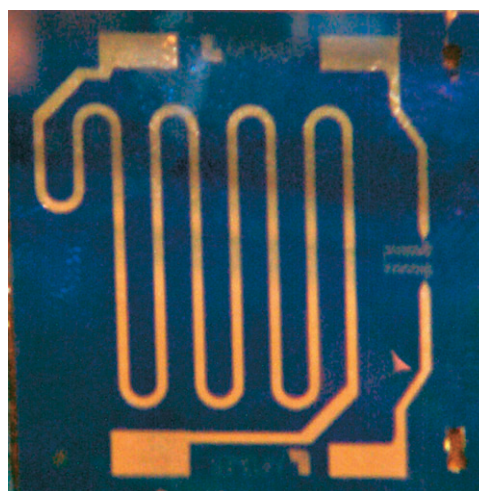
The objective of this project is to demonstrate the feasibility of a packaged microfluidic fuel processor with improved catalyst and integrated thermal management for waste-heat recovery or heat conservation through improved arrangements of heat exchanger and insulation. The project combines experimentation with theoretical and numerical analysis, design, and development and leverages LLNL's expertise in microfluidic devices, microfabrication techniques, and materials science. By delivering a reliable, long-lasting, miniature power source for military and intelligence applications such as sensors—a field in which long-lasting power sources are greatly needed—this work supports LLNL's national security mission. Farther in the future, applications could include long-lasting, lightweight power sources for a wide range of consumer electronics products, such as cell phones and laptop computers.

The power supply we are developing is a catalytic microchannel reactor based on the steam reforming of methanol, in which a mixture of water (H₂O) and methanol (CH₃OH) is heated to produce hydrogen gas (H₂) and carbon dioxide (CO₂) at ~300°C in the following reaction: CH₃OH + H₂O → CO₂ + 3 H₂. [Some methanol decomposes into carbon monoxide and hydrogen (CH₃OH → CO + 2 H₂), but a goal of catalyst optimization is to minimize decomposition.] The hydrogen fuel and the carbon dioxide byproduct are then delivered to the fuel cell manifold by microfluidic interconnects. With adequate catalyst surface area and applied heat, the microfluidic reformer produces hydrogen with only minimal power input needed to sustain the reaction. This system is thus an integrated solution that solves the issues of fuel storage, processing, and delivery.

In FY02, we developed reactor models based on published kinetics, achieving excellent agreement with our data, performed experiments using our microreactor (see figure) with two commercial catalysts containing

copper oxide (CuO) and zinc oxide (ZnO) on alumina (Al₂O₃) and achieved methanol conversion rates of 80 to 96% at 250 to 300°C, which corresponds to electrical power of 500 to 1000 mW; successfully deposited sputter-coated nickel (Ni) and CuO catalysts on microchannels and nanoporous membranes; and built and operated a PEM fuel cell fed directly by the reformat hydrogen gas and yielding up to 150 mW of electrical power—our goal is to exceed 500 mW. Byproducts of this work to date are techniques for depositing active catalysts on micro-devices and metallic sponges with very high surface area, which may be excellent catalysts for some applications. Other byproducts will include methods for feeding microreactors with very small but steady flow rates of liquid fuel, and methods to obtain very large thermal gradients external to the integrated devices. The results of this project were featured in two conference presentations, will soon appear in several peer-reviewed journals, and are expected to lead to one or more patents.

Our key objective for FY03 is to determine the best components and design for our microfluidic fuel processor so that a preprototype power module can be developed. For example, the appropriate catalyst (Ni or CuO/ZnO) and reactor configuration (microchannel, nanoporous membrane, or a combination of the two) will be chosen. Our project will also investigate how best to implement the thermal integration between the reactor inlet and the outlet, as well as how to integrate our microreactor with an operating fuel cell. 



Photograph of a microreactor (approximately 1 in. square) capable of converting a liquid fuel such as methanol to hydrogen. Using a commercially available copper oxide-zinc oxide catalyst, the microreactor achieved energy conversion rates of 80 to 96% at 250 to 300°C, which corresponds to electrical power of 500 to 1000 mW.

Nanoscale Fabrication of Mesoscale Objects

R. P. Mariella Jr., A. Rubenchik, G. Gilmer, M. Shirk

High-energy-density experiments (HEDE) are expected to play an important role in corroborating the improved Advanced Simulation and Computing (ASCI) physics codes that underlie the Stockpile Stewardship Program. To conduct these experiments, several improvements are needed—both in the diagnostics for measuring experimental results and in target fabrication. This project is working on a new LLNL capability for improving fabrication and characterization of mesoscale (millimeter size) objects with micrometer-size features at nanometer-scale accuracy for HEDE targets. Other applications include pinholes required for a phase-shifting diffraction interferometer, microporous electrodes in miniature fuel cells, remote sensors, and medical technologies. To create a fabrication capability that is deterministic, this research combines modeling and experiments.

This project leverages LLNL expertise in modeling, simulation, and laser-surface interactions to develop a new capability for fabricating and characterizing mesoscale targets for weapons physics experiments in support of LLNL's stockpile stewardship mission.

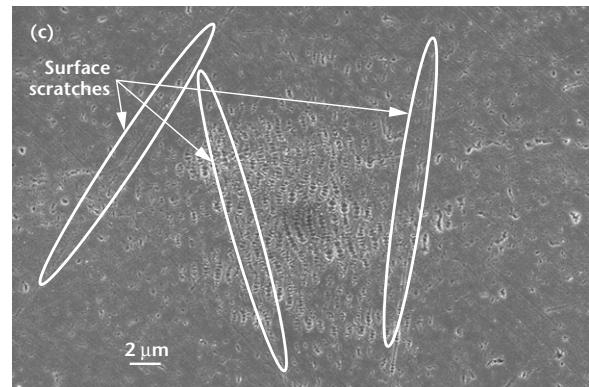
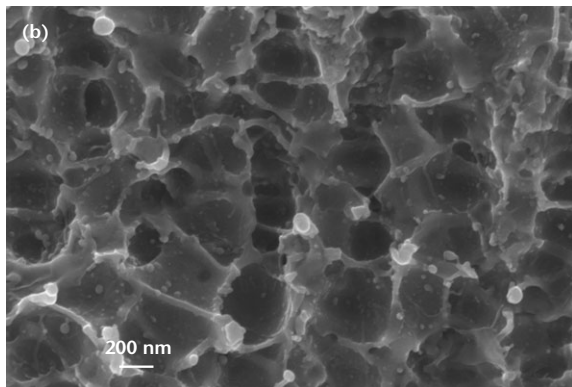
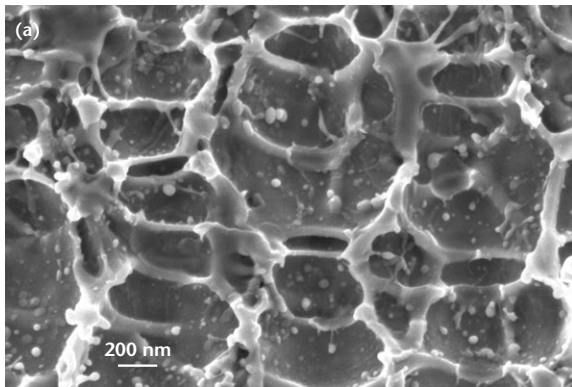
In FY02, we successfully combined three-dimensional (3-D) molecular dynamics (MD) modeling with the 1-D hydrocode, HYADES to take advantage of the strengths of each approach. First, the laser-material

interaction with HYADES is tracked. Then, well after laser pulse termination and the relaxation of the electron subsystem, the density, velocity, pressure and temperature profiles are passed on as initial conditions for the MD simulator. For 150-fs laser pulses on copper, this approach predicts void nucleation to occur within about 20 nm of the surface.

Experimentally, our studies included single-shot and multiple-shot ablation of single-crystal and polycrystalline, copper and gold targets, using 150-fs laser pulses at 800-nm wavelength. For laser pulses only slightly above the threshold for ablation, results show that the residual surface roughness is relatively independent of the total depth of the ablation crater [Figs. (a) and (b)]. We have also observed that initial surface scratches, like those in Fig. (c), tend to be nucleation sites for the micropits that are formed during ablation. During FY03, we plan to continue exploring the possibility of using submicrometer-spaced ridges, made by diamond turning of the surface prior to laser ablation, to "seed" and control the growth of these features.

Laser "polishing" could reduce the amplitude of sub-micrometer surface perturbations caused by ablation, without affecting the longer-length-scale pattern formed by this process. Using a Monte Carlo model of the crystal surface structure, we studied the effect of laser heating the object to temperatures near the melting point. Though effective, the time required was too great for efficient processing. However, by modeling laser pulses that produce a transient liquid layer of controlled thickness (surface melting), we predict that the time required to smooth the surface could be reduced dramatically. The trade-off between the smoothing and freezing times determines the duration, period, and intensity of the polishing pulses.

In FY03, we plan to use diamond-turned copper, gold, and nickel substrates to study the smoothing processes experimentally with excimer laser pulses at 193 nm.



Photomicrographs of copper surfaces, showing little difference in surface roughness after ablation with (a) 5 and (b) 100 150-fs laser pulses at 800 nm. Microscale pock marks are seen in (c), some nucleating on initial surface scratches.

Low-Voltage Spatial Light Modulator

A. P. Papavasiliou


Spatial light modulators (SLMs) are electro-optic devices for modulating the phase, amplitude or angle of light beams. Applications for arrays of SLMs include turbulence correction for high-speed optical communications, imaging through distorting media, input devices for holographic memories, optical manipulation of DNA molecules, and optical computers. Devices based on microelectromechanical systems (MEMS) technology have recently attracted special interest because of their potential for greatly improved performance at a much lower cost than liquid-crystal-based devices. The new MEMS-based SLM devices could have important applications in high-speed optical communication and remote optical sensing in support of DoD and DOE national security missions.

Present MEMS SLMs are based on parallel-plate capacitors where an applied voltage causes a suspended electrode to move towards a fixed electrode. They require relatively high voltages, typically on the order of 100 V, resulting in 1) large transistor sizes, available only from specialized foundries at significant cost, and which limit the amount and sophistication of electronics under each SLM pixel; and 2) large power dissipation per area, which requires heat removal due to the optical precision required ($\sim 1/50$ of a wavelength).

This project studied the feasibility of a three-electrode actuator technology that promises to reduce the

switched voltage requirements and linearize the response of spatial light modulators. By adding a third electrode and the ability to tune nonlinear springs our SLM design can reduce the required switched voltage and increase the linearity of the voltage-displacement response.

In FY02, we achieved three major technical goals: 1) developed computer models that demonstrate substantial advantages offered by this technology (Fig. 1); 2) determined a fabrication method and optimal designs for test devices; and 3) fabricated and tested those devices. Figure 2 is a microphotograph of the three-electrode actuator.

The computer models we developed demonstrate the advantages of the three-electrode actuator in comparison to the conventional parallel-plate actuator. Displacements comparable to the conventional actuator are possible with less than one-third of the switched voltage, and the voltage-displacement characteristics are significantly more linear. Using the computer model and optimal design techniques, we created designs for test structures that maximize linearity and can be fabricated in a standard MEMS foundry process. We had parts fabricated and tested those parts. The results show that the actuators behave as predicted: increasing bias voltage on the third electrode increases linearity and reduces required switched voltage. 

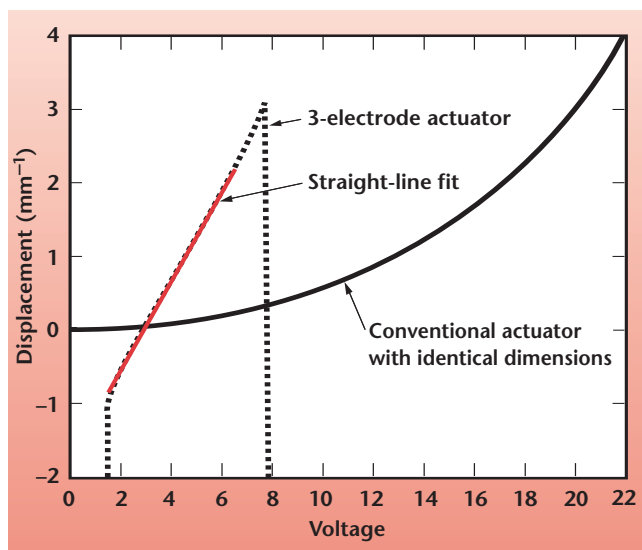


Figure 1. Plot of simulated actuator response.

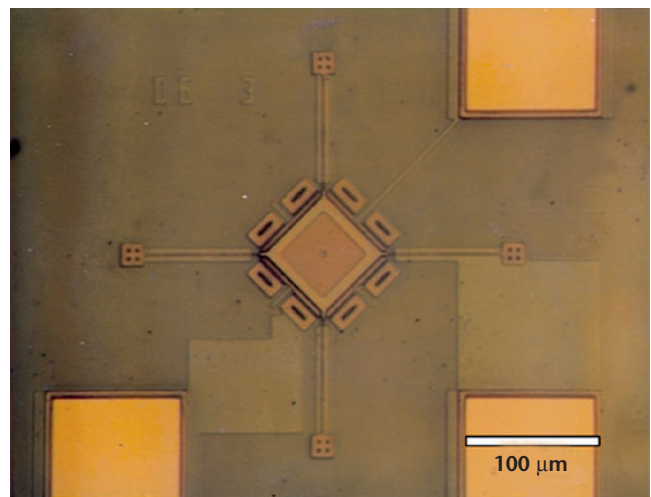
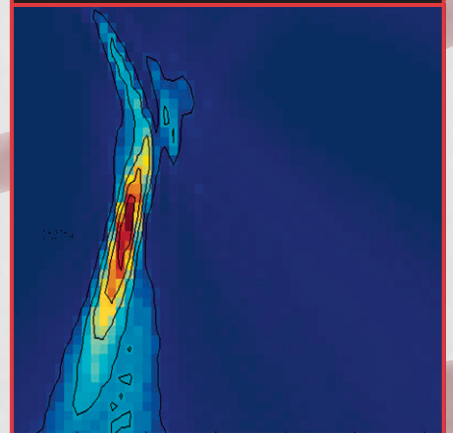
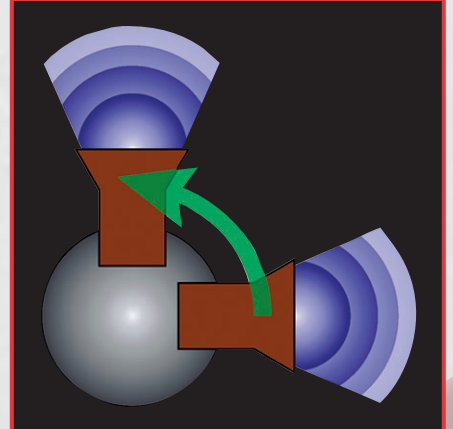


Figure 2. Photograph of actuator.

Center for Nondestructive Characterization



High-Accuracy X-Ray Imaging of High-Energy-Density Physics Targets

W. Nederbragt, D. Schneberk, T. Barbee, J. L. Klingmann, S. G. Lane, J. A. Jackson

High-energy-density experiments play an important role in corroborating the improved physics codes that underlie LLNL's stockpile stewardship mission. Conducting these experiments will require improvements in diagnostics, in fabrication techniques, and especially in characterizing the target assemblies, which have millimeter-sized components with micrometer-sized features.

X-ray microscopy and tomography hold promise for characterizing the internal structure of target assemblies. Submicrometer spatial resolution has been demonstrated using a synchrotron x-ray source, but that approach does not accommodate LLNL's requirements for a high-throughput, low-cost approach for characterizing production quantities of target assemblies.

This project is conducting the research and development of an x-ray microscope that uses a replicated multilayer Wölter Type-I optic. The fabrication of the optic is the key to the project's success. The replication technique coats a superpolished mandrel (see figure) with reflective multilayer materials. The multilayers are covered with a 1- to 2-mm-thick layer of nickel to provide structural rigidity. The Wölter optic is then separated from the mandrel. This results in an optic with nearly the same figure and roughness as the mandrel. If successful, this microscope will provide high-throughput and high-resolution x-ray imaging of target assemblies in a laboratory setting. Moreover, this instrument would bring a new capability to the Laboratory that will have application to stockpile stewardship and a variety of other mission areas.

During FY02, we designed the optical system, simulated the three-dimensional x-ray imaging properties of our optical design, and fabricated mandrels for creating the optics.

The optical design involved an extensive parameter study to determine the best design for our needs. Parameters included the maximum reflection angle, length, magnification, and collection efficiency (photon

throughput) of the instrument. The maximum reflection angle was influenced by the use of multilayer technology, which was incorporated into our optical design. The result of the optical analysis was a microscope design with a length of 5 m, a magnification of 12 \times , and a solid collection angle of 0.0019 sr.

With the optical design complete, we constructed a test mandrel for testing and adjusting the multilayer coating process. Several more test mandrels were fabricated and used to test the mandrel-optic separation process.

The super-polished mandrel has been fabricated, coated with nickel, and diamond-turned to get the surface figure to less than 25 nm. After completing the diamond-turning process, the mandrels were superpolished to 3 to 5 Å. One mandrel can be used to fabricate several optics.

In FY03, we will complete the mechanical design of the prototype microscope, fabricate several optics using the superpolished mandrel, construct the prototype microscope, and test the microscope using phantoms (test parts) and real target assemblies. If the project succeeds, this instrument will lead to the construction of a production microscope.



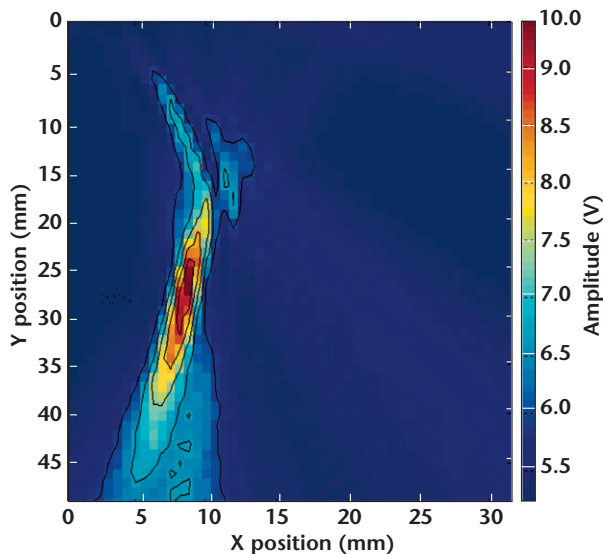
Diamond turning of the high-accuracy mandrel.

Ultrasonic Nondestructive Evaluation of Multilayered Structures

M. J. Quarry, K. A. Fisher, J. L. Rose

Multi-layered structures such as weapons assemblies and aircraft wings pose challenges for nondestructive evaluation (NDE) techniques—to detect a cracked ceramic or void in a multi-layered weapons system, for instance—because of inaccessible areas and close interfaces. We are developing two approaches for overcoming these difficulties: 1) guided-wave modes and 2) beam steering of bulk waves.

The first approach involves using the wave-guide structure of a multi-layered medium to send wave modes along the structure into inaccessible areas, and requires the ability to preferentially excite modes in which most of the energy exists in the layer of interest. A novel phased-array method is being developed under this project to find such guided-wave modes experimentally. Most guided-wave research has been limited to single layers, such as aluminum plates in aircraft or steel piping. Investigating guided waves in multilayered media will extend guided-wave techniques into many new applications.




An imaged section of an aluminum block with a 1-mm-diameter side-drilled hole obtained by a 20°-ultrasonic steered beam.

The second approach steers and focuses ultrasonic bulk waves into layers of interest to find voids in a sub-layer. Steering the beam enables areas up to ~6 in. to be scanned from a single position. Focusing increases resolution and improves minimum flaw-size detection.

Our project will develop advanced technologies for inspecting weapons systems in support of LLNL's stockpile stewardship mission and will establish the science base for using guided-wave-based NDE for multilayered mesoscale targets.

In FY02, a model of guided-wave mode generation by phased array was developed. Results of analysis using this model showed the need to maximize array length, minimize the effect of element spacing, and maximize the number of elements. We then designed an array based on this analysis and used it to detect successfully a 30% through-wall notch in a 1/8-in.-thick aluminum plate, although sensitivity was ~33% less than that of traditional ultrasound.

We developed a software interface for steering a phased array of ultrasonic beams for single-layer media. In addition, a time-delay beam image reconstruction algorithm previously developed at LLNL for steered-beam data was modified and used to image a 1-mm-diameter hole in an aluminum block—achieving our goal of detecting flaws of 1 mm in diameter. The area of the block shown in the figure was imaged by focusing the 20°-off-axis beam at the center of the area.

In FY03, we will advance from single-layer to multilayered media and 1) perform proof-of-concept testing of guided waves and bulk waves for the NDE of multilayered structures by detecting programmed flaws in multilayered structures; 2) develop array input parameters for beam steering in multilayered media; 3) modify image reconstruction codes for multilayered media; and 4) improve axial distortion in images. 

Radial Reflection Diffraction Tomography

S. K. Lehman, S. J. Norton


Consider a wave-based measurement system (either acoustic or electromagnetic) in which a single transducer rotates about a fixed radius in a “pitch-catch” multimono-static mode, *i.e.*, at each successive angular location about its center, the transducer launches a field into its surrounding medium (the pitch) and subsequently records the backscattered field from that medium (the catch) (see figure). We developed a diffraction tomography (DT) algorithm, a technique based on a linearized version of the forward field-scattering equation, to form planar slice images of the medium surrounding the transducer. The theory and imaging technique are referred to as radial reflection diffraction tomography (RRDT) because of the radial configuration of the transducer and the tomographic paradigm used to reconstruct the structure of the surrounding medium from reflected waves.

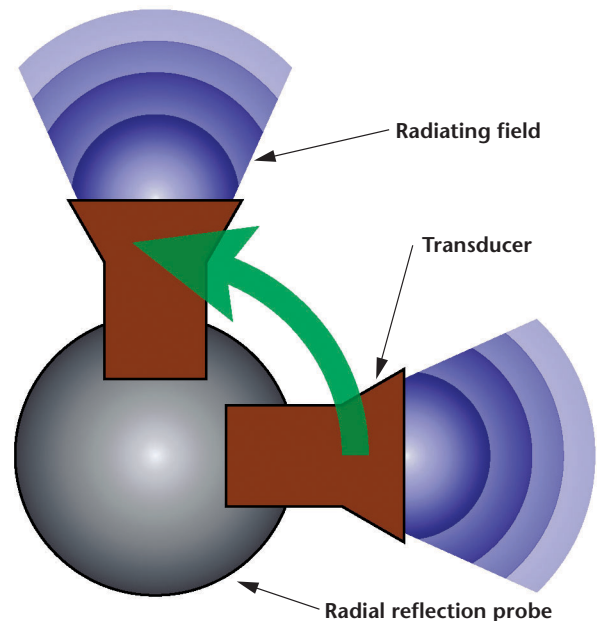
As a minimally invasive nondestructive evaluation tool, RRDT has the potential to improve intravascular ultrasound techniques used for imaging plaque buildup on arterial walls. It also has applications to the Laboratory’s stockpile stewardship mission.

Our forward field-scattering equation and inversion algorithm are based on a 2.5-dimensional scattering model in which the medium does not vary in the third (or z) dimension. This is a reasonable approximation, given the goal of achieving planar reconstructions. During development of the theory, we discovered that it is not mathematically possible to reconstruct fully complex images, *i.e.*, maps for both object velocity and attenuation; only velocity maps can be achieved.

Under the constraint that the object function is real, we successfully derived an inversion expression that reconstructs planar velocity slices of the object and the Fourier Diffraction Theorem for this geometry, which dictates the resolution limit of the reconstruction. Numerical implementation of the inversion algorithm, however, has been hindered by the existence of a reciprocal of a Bessel function of the first kind in the

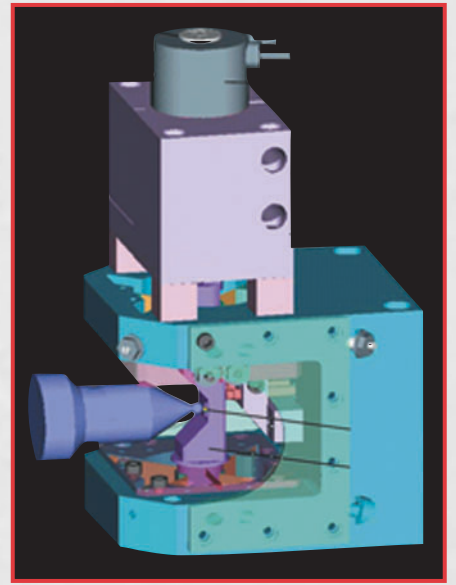
integrand of the inversion integral. The multiple zeros of the Bessel function cause the integrand to diverge. These Bessel function zeros in the denominator can be viewed as poles along the real axis and it is natural to attempt a complex integration, replacing the integral by the sum of the integrand residues at the poles. We derived and implemented such a method but have not yet had success at forming images due to the behavior of the some of the terms in the integrand in the complex plane.

In FY03, we will develop a numerical inversion method based on a recently derived generalized tomographic inversion method that can be easily implemented numerically. This fully complex inversion method will yield reconstructions of both sound speed and attenuation. 



Radial reflection probe with the transducer shown launching a field at two angular locations.

Center for Precision Engineering



Extremely High-Bandwidth, Diamond-Tool Axis for Weapons-Physics Target Fabrication

R. C. Montesanti, D. L. Trumper, J. L. Klingmann

Our project will enable the fabrication of high-contour accuracy and low-roughness three-dimensional (3-D) target features for weapons-physics experiments using high-power lasers by expanding the bandwidth of a fast-tool-servo (FTS) axis to 10 kHz. This work will build on recent research efforts in the area of rotary-motion FTSs. Current capabilities are limited for fabricating 3-D target features, which are used to investigate weapons performance characteristics. At present, ultraprecise, single-point diamond-turning machining methods are the most accurate and efficient approach for fabricating certain target features, such as the longest spatial wavelengths of surface contours. These methods also offer the lowest risk for implementation.

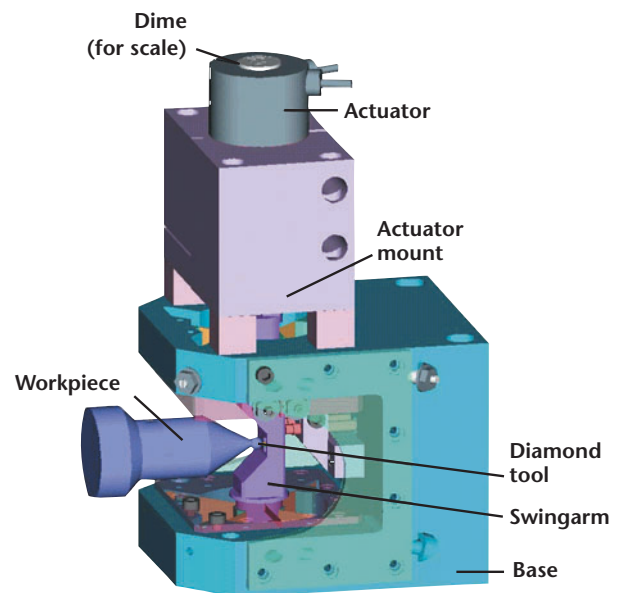
This project proposes to develop a 10-kHz FTS—a short stroke, fast moving machine axis that can be coupled with precision machines to create a unit that will enable us to use single-point machining to produce higher spatial-frequency surfaces while maintaining very high accuracy. A rotary FTS design was chosen because the reaction torque is more easily managed than a linear force equivalent.

Initially we plan to develop a 2-kHz prototype FTS that will include a commercially available actuator. This approach will allow us to address high-risk controller issues associated with cutting dynamics and provide a system for target fabrication early in the project cycle. Once this first unit meets our desired specifications (a 2-kHz bandwidth with accurate motion control to $0.5\ \mu\text{m}$ and high stiffness of $18\ \text{N}/\mu\text{m}$), knowledge gained from this work will enable us to fabricate physics-target components that are beyond the reach of current fabrication technology. In addition, by expanding the bandwidth of this type of mechatronic device, our new unit will advance the state of the art in the precision-mechatronic field.

During FY02 we designed a mechanism for the 2-kHz FTS. The system includes an innovative (patent

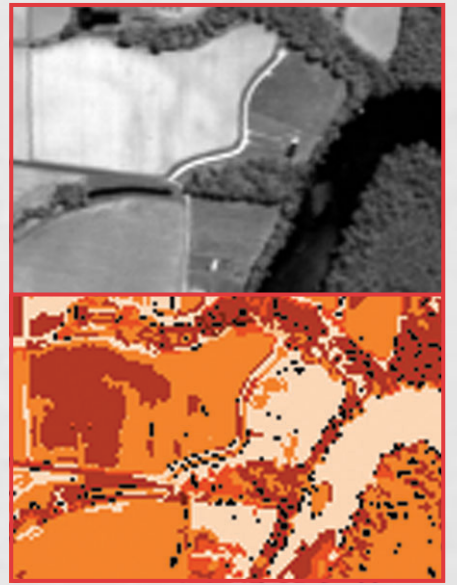
application in process) rotary architecture that minimizes disturbance forces and torques on diamond-turning machines used for target fabrication and a device that provides guided motion for the FTS while maintaining the stiffness needed for diamond turning. We also ordered fabrication of all parts, purchased a 2-kHz commercial galvanometer integrated with a digital controller, and developed a detailed design package for the 2-kHz FTS and sophisticated control algorithms.

In FY03, we will assemble and integrate the mechanism for the 2-kHz system with the galvanometer and digital controller, operate the system in a closed-loop manner, refine the control algorithms, integrate the system with a diamond-turning machine at MIT to produce test parts, and develop an advanced actuator. The system will be transferred to LLNL by the end of the year.



Computer-aided design of the 2-kHz fast-tool servo.

Other Technologies



Hyperspectral Image-Based Broad-Area Search

D. W. Paglieroni

From the standpoint of the national security and non-proliferation missions of LLNL, two of the most important tasks faced by human image analysts are broad-area search (reconnaissance) and site monitoring (surveillance). In each, the objective is to detect targets of interest—typically solid, manmade objects such as buildings and moving vehicles or gaseous phenomena such as plumes. A broad-area search involves static images of large swaths of land, whereas site monitoring involves analyzing smaller images in a time sequence. Detection is often a time-critical task in which image analysts face growing volumes of image data collected with increasingly sophisticated imaging sensors.

Hyperspectral (multiband) images consist of hundreds of single-band images stacked on top of one another, each corresponding to a different frequency band. They provide a much greater context for both spatial and spectral signatures than conventional single-band images, and are potentially far more useful for broad-area search and site monitoring. Unfortunately, image analysts do not always have time to analyze all the conventional single-band imagery presented to them, let alone voluminous hyperspectral imagery.

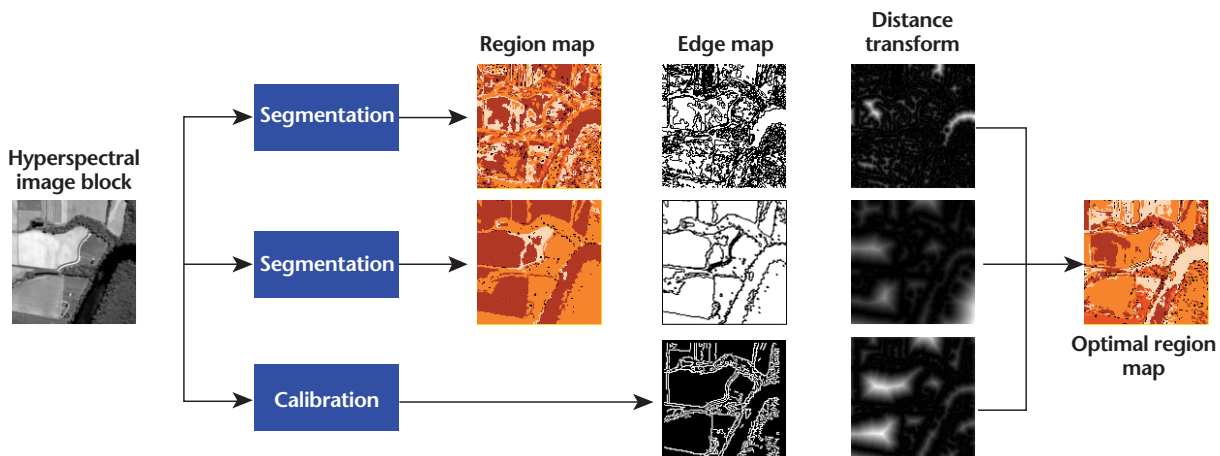
The goal of our hyperspectral image-based broad-area search (HIBAS) project is to improve image analysis throughput, without sacrificing detection performance, by developing and testing fast image-analysis algorithms that extract objects from images, allowing image analysts to focus on regions containing objects matching the target's properties. The algorithms process large images one block at a time and comprise two types: 1) segmentation algorithms, which first divide images into regions containing pixels that are clustered together—suggesting a single

object—and 2) spatial-signature-analysis algorithms, which then detect regions or groups of connected regions that have spatial properties similar to the target.

In FY02, we found that image-segmentation quality is affected as much by algorithm parameters as by choice of algorithm. Rather than developing a fundamentally new segmentation algorithm, we developed a generic self-calibration process that applies to many segmentation algorithms and that can automatically determine the parameter settings that produce the best result (see figure). The self-calibration process was applied in experiments on a number of hyperspectral images from different sensors using two core-segmentation algorithms: 1) a region-growing algorithm that grows regions from seed pixels in accordance with a spectral homogeneity constraint parameter; and 2) the K-Means Re-Clustering algorithm, which automatically groups pixels into one of several spectral classes that are learned automatically, according to a parameter that specifies the number of classes.

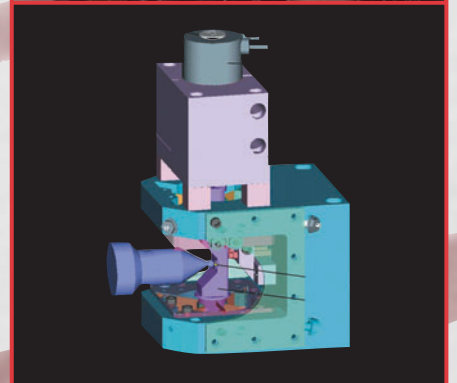
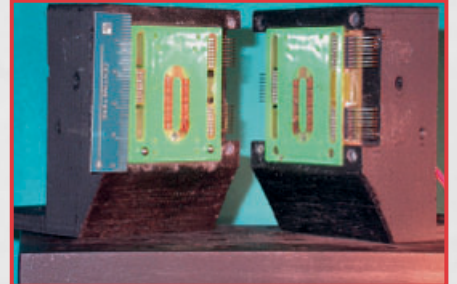
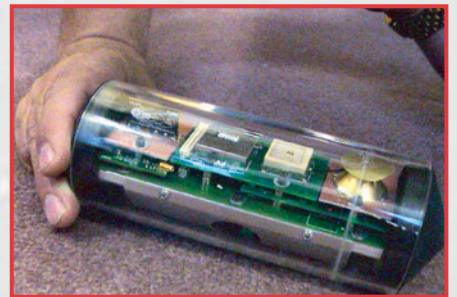
An algorithm and an efficient implementation for spatial signature analysis based on area correlation were developed; these have potential applications to detecting objects of known shape in remotely sensed imagery and gas plumes in matched, filtered images.

The HIBAS spatial-signature-analysis algorithms developed in this project apply to various problems related to national security and nonproliferation. Issues remaining include image-segmentation algorithms that are free of problematic parameters whose values are difficult to set, model-based signature analysis techniques for detection of objects with known physical models, and more flexible spatial-signature-analysis techniques capable of detecting objects of known shape.



Graphical depiction of our self-calibration process for image segmentation. A hyperspectral image is segmented by a core-segmentation algorithm with different parameter settings, such as a region grower with a region homogeneity parameter. Each parameter setting has an associated region map whose borders are compared to edges independently extracted for calibration. The distance transform captures the distance from each pixel to the nearest edge pixel. The parameter setting for which the region boundaries most closely match the calibration edges is used.

Author Index



Author Index

| | | | |
|-----------------------------|--------|-----------------------------|--------|
| Armstrong, G. H. | 3 | Mish, K. D. | 12 |
| Barbee, T. | 25 | Montesanti, R. C. | 31 |
| Becker, R. | 13 | Morse, J. D. | 20 |
| Behymer, E. M. | 17 | Myers, S. C. | 5 |
| Benett, W. | 19 | Nederbragt, W. | 25 |
| Bennett, C. V. | 17 | Nelson, K. E. | 5 |
| Benzel, D. | 4 | Ness, K. D. | 14, 19 |
| Bond, S. W. | 17 | Norton, S. J. | 27 |
| Bond, T. C. | 18 | Paglieroni, D. W. | 35 |
| Champagne, N. J. | 9, 11 | Papavasiliou, A. P. | 22 |
| Chen, A. | 19 | Puso, M. A. | 10 |
| Christian, A. | 19 | Quarry, M. J. | 26 |
| Clague, D. S. | 14 | Richards, J. | 19 |
| Dowla, F. | 4 | Roberts, R. S. | 3 |
| Fisher, K. A. | 26 | Rodgers, A. J. | 6 |
| Gilmer, G. | 21 | Rose, J. L. | 26 |
| Han, I. Y. | 17 | Rosenbury, T. | 4 |
| Harben, P. E. | 5 | Rubenchik, A. | 21 |
| Harris, D. B. | 5 | Schneberk, D. | 25 |
| Havstad, M. A. | 20 | Sharpe, R. M. | 9, 12 |
| Jackson, J. A. | 25 | Shirk, M. | 21 |
| Jankowski, A. F. | 20 | Sperry, V. R. | 17 |
| Jones, E. D. | 3 | Spiridon, A. | 4 |
| Kallman, J. K. | 18 | Stowell, M. | 9 |
| Kent, K. A. | 3 | Stratton, P. | 19 |
| Khanaka, G. H. | 18 | Trumper, D. L. | 31 |
| Klingmann, J. L. | 25, 31 | Upadhye, R. S. | 20 |
| Lane, S. G. | 25 | Weisgraber, T. H. | 14, 19 |
| Larsen, S. C. | 5, 6 | Welty, R. J. | 17 |
| Lehman, S. K. | 27 | Wheeler, E. K. | 19 |
| Madsen, N. K. | 11 | White, D. A. | 9, 11 |
| Mariella Jr., R. P. | 21 | Yoo, S. J. | 17 |
| McCallen, D. B. | 6 | Zywicz, E. | 10 |

Manuscript Date March 2003
Distribution Category UC-42

This report has been reproduced directly from the best available copy.

Available for a processing fee to U.S. Department of Energy and its contractors in paper from
U.S. Department of Energy
Office of Scientific and Technical Information
P.O. Box 62
Oak Ridge, TN 37831-0062
Telephone: (865) 576-8401
Facsimile: (865) 576-5728
E-mail: reports@adonis.osti.gov

Available for sale to the public from
U.S. Department of Commerce
National Technical Information Service
5285 Port Royal Road
Springfield, VA 22161
Telephone: (800) 553-6847
Facsimile: (703) 605-6900
E-mail: orders@ntis.fedworld.gov
Online ordering: <http://www.ntis.gov/products/>

Or

Lawrence Livermore National Laboratory
Technical Information Department's Digital Library
<http://www.llnl.gov/library/>

This document was prepared as an account of work sponsored by an agency of the United States Government. Neither the United States Government nor the University of California nor any of their employees, makes any warranty, express or implied, or assumes any legal liability or responsibility for the accuracy, completeness, or usefulness of any information, apparatus, product, or process disclosed, or represents that its use would not infringe privately owned rights. Reference herein to any specific commercial products, process, or service by trade name, trademark, manufacturer, or otherwise, does not necessarily constitute or imply its endorsement, recommendation, or favoring by the United States Government or the University of California. The views and opinions of authors expressed herein do not necessarily state or reflect those of the United States Government or the University of California, and shall not be used for advertising or product endorsement purposes.

This work was performed under the auspices of the U.S. Department of Energy by the University of California, Lawrence Livermore National Laboratory under Contract W-7405-Eng-48.
ENG-02-0143-AD



**Lawrence Livermore National Laboratory
University of California
P.O. Box 808, L-124
Livermore, California 94551**

http://www_eng.llnl.gov/

